CHAPTER **4**

Back-analysis and optimisation

1. Introduction

This chapter aims to describe the main principles of the back-analysis applied to the resolution of the dynamic pile testing analysis. This process is the main tool used to extract the parameters of the pile/soil interaction system from the dynamic measurements obtained in the field.

The general principle followed is described including the type of data involved in the process, the quality criterion leading the optimisation, the details of the analysis in the duration and pile/soil characterization and the way used to visualize the results of the optimisation. Afterwards, an automatic method of matching is presented, described and validated with a short analysis of the uniqueness of the obtained solution. Some guides are also given to accelerate, improve or validate the matching procedure. The matching procedure and the back-analysis works with a variable set of parameters. Within this group, some parameters have a larger influence compared to others. A section is dedicated to the sensitivity analysis allowing to classify the parameters and to use this classification to improve the reliability of the back-analysis. Finally, a sequence of dynamic load tests from Sint-Katelijne-Waver and Limelette are analysed .

2. The back-analysis system used in the dynamic pile testing analysis

2.1. Principle

The main principle of the back analysis uses the fact that the pile/soil model described in chapter 3 is able to calculate the system response for a given impetus. This input signal is an event measured during the dynamic test. The pile response is compared to the measured one and the gap between curves is considered as a measure of the imperfection ofthe simulation. The smaller the difference, the best the calculated response. Consequently, if the pile/soil interaction is known, simulations of other solicitations are possible (like Static load settlement curve).

The main goal of the technique is to adjust the parameters characterizing the pile/soil model chosen in order to fulfil a criterion based on the measured data issued from the dynamic test. When the criterion is achieved, the model is considered as describing the pile/soil system. The criterion commonly used by numerous procedures works with the force or velocity signal as input and control data of the matching procedure. The procedure follows those steps:

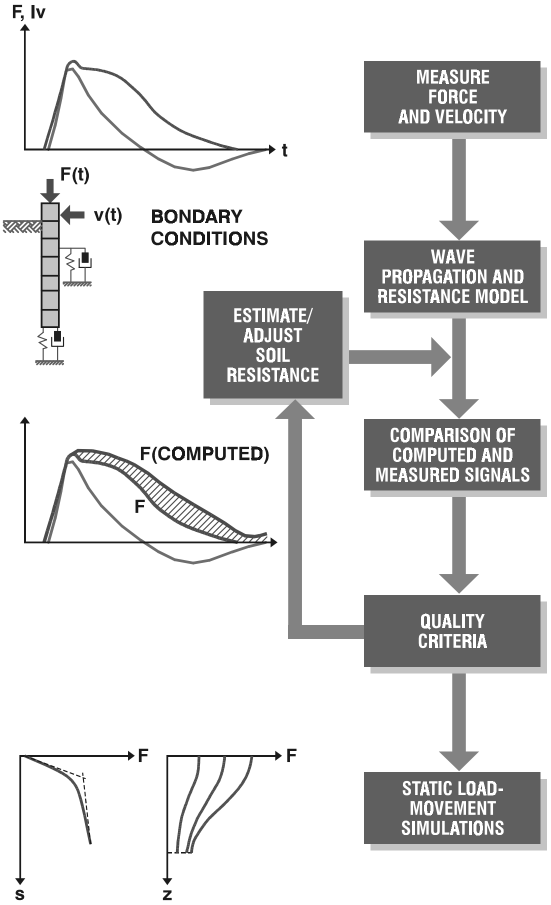

Figure IV-1 : NUSUMS procedure (Holeyman, 1992)

- Either the force or the velocity[1] is imposed as a stimulus at a boundary of the model;

- The model uses this stimulus and calculates the pile/soil response. Either the velocity (if the force is used as stimulus) or the force (if the velocity is used as stimulus) is calculated;

- The computed signal and the measured signal (not used as a stimulus) are compared and a quality criterion determines the degree of agreement between both signals;

- If the matching agrees, the procedure is stopped and the used parameters are considered to describe the pile/soil model for the analysed test in the configuration of the chosen model;

- If the quality criterion does not fulfil the requirements of agreement, the model parameters are re-estimated and a new loop is launched in order to improve the matching agreement.

Figure IV-1 describes the resolution algorithm and is called NUMSUMS for NUMerical Simulations Using Measured Signals.

The present chapter describes the improvements brought during this research to this important step of the analysis and this particular section aims to describe the general tools and characteristics of the back-analysis process.

[1] Or a combination of signals like the downwards and the upwards forces waves

2.2. Used signals and quality criterion

The dynamic measurements are of two types: the dynamic (the strain (force) at the pile head) and the kinetic (the acceleration (velocity) at the pile head) ones. Both of them are incorporated in the back analysis process. These signals can be used either as input or as reference for the comparison step. If the force is imposed as boundary condition, the velocity of the pile head is calculated and compared to the measured one, while if the velocity is chosen as impetus, the force is used as reference for the comparison and the matching quality evaluation.

It is also possible to mix the force and the velocity signals in order to impose the downwards wave and to compute the upwards wave to be compared with the measured upwards wave.

The force and velocity data are measured independently with transducers (strain gage and accelerometers). When the fitting between curves is achieved by using one signal as input and the other as reference, the simple fact to invert the signals used as input is a check of the quality of the result.

Both signals are imposed as boundary condition and as reference. The average gap between the measured and calculated curves is evaluated for both couples of curves and their sum represents the general quality criterion to be minimized. By this way, the crossing check is realized each time and the set of parameters giving the best fit between curves optimises both possible approaches (force or velocity imposed to the system):

$$D_p = D_{pF} + D_{pV}$$ **Equ. IV- 1**

Where:

- D_{pV} is the normalized average gap between the measured and calculated velocity traces;
- D_{pF} is the normalized average gap between the measured and calculated force traces;
- D_p is the normalized gap equal to the sum of both normalized distances of the force and velocity signals and considered as the quality criterion.

D_p means normalised gap for the set of parameters p, as follows:

$$D_{pV} = \frac{\sum_t (V_m - V_c)^2}{\sum_t (V_m)^2} \quad [\%]$$ **Equ. IV- 2**

$$D_{pF} = \frac{\sum_t (F_m - F_c)^2}{\sum_t (F_m)^2} \quad [\%]$$ **Equ. IV- 3**

F_m is the discrete measurement of force; V_c is the discrete calculation of velocity;

F_c is the discrete calculation of force; t is the duration of the analysis.

V_m is the discrete measurement of velocity;

Figure IV-2 and Figure IV-3 provide the result of an optimisation. The shaded zones represent the gap between curves to be minimized.

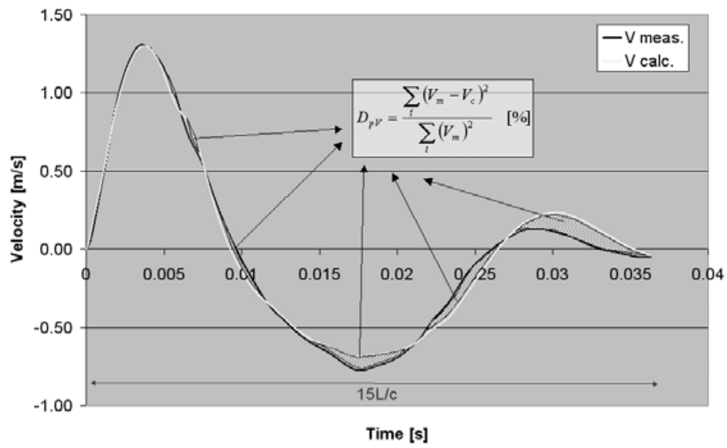

Figure IV-2 : Measured and calculated velocity signal

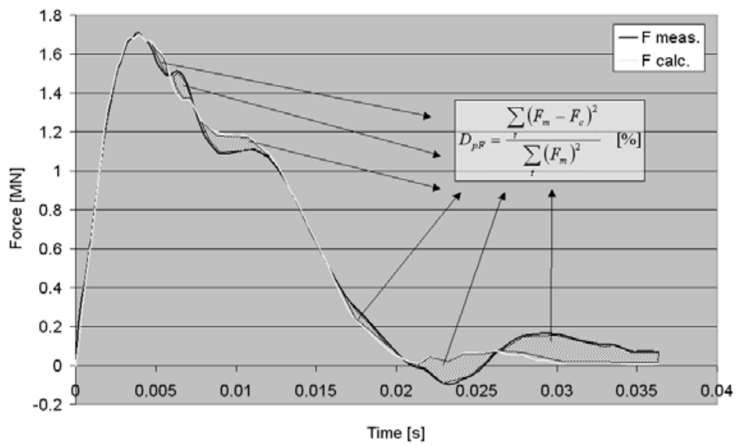

Figure IV-3 : Measured and calculated force signal

The gap is normalized in order to allow the sum of the gaps between signals of different units (force or velocity) and to allow comparison of analysis performed on tests of different energy (drop heights increasing → vel and force increasing). The square function is applied to avoid the negative values problem. This has an influence on the evaluation of the best solution. The minimization of this function favours the decreases of the higher gaps in comparison to the smaller ones (because of their higher relative weight in the general sum).

Others methods of gap evaluation exist in the literature:

- The automatic matching procedure of CAPWAP® described in Rausche et al. (2000) uses a normalized and weighted sum of the difference existing between both measured and calculated curves. The purpose is to minimize this value by changing the parameters.

$$D_C = \min \sum_t |Dif| = \int_t |F_m - F_c| \cdot dt$$ **Equ. IV- 4**

The normalization is made with respect to the temporal integration of F_m. The match over a period of 3ms following the first return of the stress wave from the pile toe is given a double weight in the summation because of its importance for a total capacity determination.

- El Naggar and Baldineli (1998) minimize the squared difference between computed and measured displacements (ΔD):

$$D_{EN} = \min \sum_t \left[\frac{D_c - D_m}{D_m}\right]^2$$ **Equ. IV- 5**

This is almost the same formulation than the one presented in this section, but the use of the quotient inside of the summation includes high risks of divergences when the discrete value of D_m is close to 0.

- Berzi (1994, 1996, 1999) defines the observed and the simulated system responses as represented by two curves in a 2-D system and by m discrete points (1, …, m) with coordinates x_i and y_i (I = 1 to m). The deviation between both curves is quantified by the area Dp equal to the sum of the partial area r(p). The partial area is defined as the area of the quadrangle among the j-1th and the jth point (j < m) (Figure IV-4). The areas are evaluated in a normalized coordinate system: gap

$$\begin{bmatrix}(x)\\(y)\end{bmatrix} = \begin{bmatrix}\dfrac{x - x_{\min}}{x^0_{\max} - x^0_{\min}} \cdot W \\ \dfrac{y - y_{\min}}{y^0_{\max} - y^0_{\min}} \cdot \dfrac{1}{W}\end{bmatrix}$$ **Equ. IV- 6**

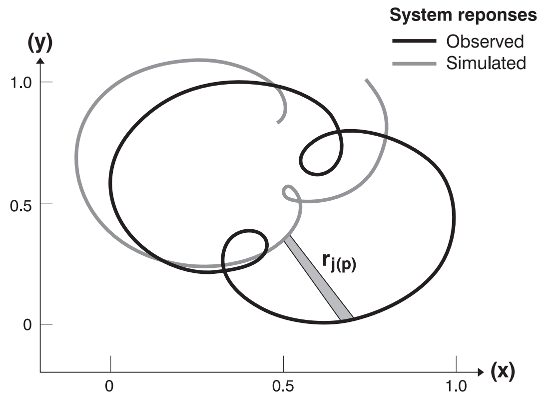

Figure IV-4 : Definition of the distance between system responses (after Berzi, 1999)

$x_{min,max}$ are the min and max values of the x coordinates; The term W is a weight factor;

$y_{min,max}$ are the min and max values of the y coordinates; (x) and (y) are the normalized coordinates.

the superscript "0" referred to the observed response;

The quality criterion becomes:

$$D_B = \min \sum_i^{1\to m} |r_i(p)|$$ **Equ. IV- 7**

- TNOWAVE® uses also an automatic matching procedure but the authors do not describe the quality criterion used with accuracy. The literature informs that the convergence criterion can be a small residual between calculated and measured signals, a small update for the parameters or a maximum number of iterations.

The duration of analysis has a certain influence on the value of the quality criterion. All signals (force, velocity, …) stabilize faster or slower depending of the type of signal and the type of soil: the clay dampens the pile oscillations faster than the sand and the load signal is the shortest one compared to the acceleration, the velocity and the displacement, respectively placed in an increasing duration order.

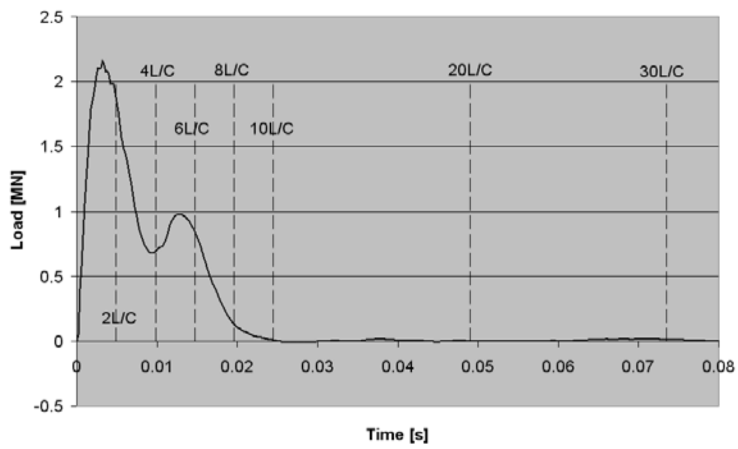

Figure IV-5 : Load signal marked with multiples of travel duration

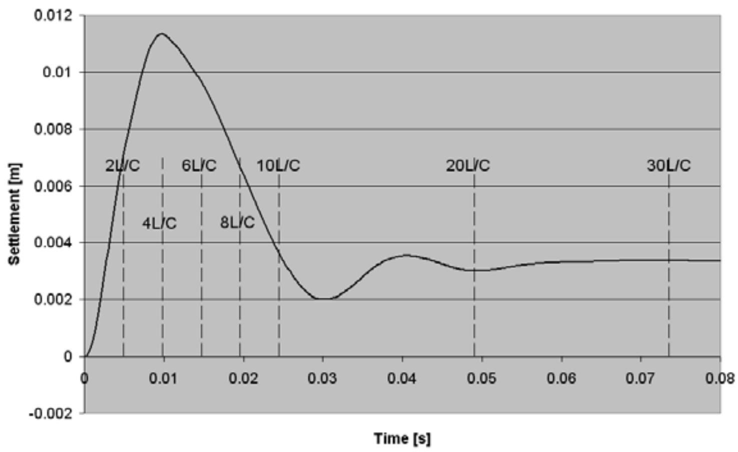

Figure IV-6 : Settlement signal marked with multiples of travel duration

Figure IV-5 and Figure IV-6 exhibit the difference existing between the load and the settlement time histories. The time determined to perform the back analysis depends on the parameters to be optimised and the time available to analyse the signals. The longest the signal to be analysed, the longest the analysis duration due to the time processing. Moreover, the first part of the signal only concerns the loading, the unloading parameters can not be optimised. Time processing management and choice of parameters to be optimised are two antagonist steps in the general process.

In the following treatments, the duration of analysis is defined by the number of travelling of the wave into the pile. The time needed to a wave to travel from the to the base is determined by the pile length (L) and the wave propagation velocity (c):

$$t = \frac{L}{c} \qquad \textbf{Equ. IV- 8}$$

Consequently, the time fixed to perform the back analysis is determined in multiple of this duration:

$$t = \frac{4L}{c}, \frac{6L}{c}, \frac{10L}{c}, \frac{20L}{c}, \ldots$$

2.3. Results and comparison of signals

The result of the optimisation is given in percent [%] (the value of D_p). But different graphical results can confirm the quality of the optimisation. The load-settlement trace is the most used in the future developments to represent the quality of the optimising procedure (Figure IV-7). This curve summarizes both measured information: force and settlement. The best optimisation must be reliable in both domains and the comparison of measured and computed curves is a good way to check the quality of the back-analysis and the potential zones of erroneous modelling.

Figure IV-7 displays the data and the three possible representations of the pile/soil response:

- The force calculated with the settlement measured;
- The force measured with the settlement calculated;
- The force calculated with the settlement calculated.

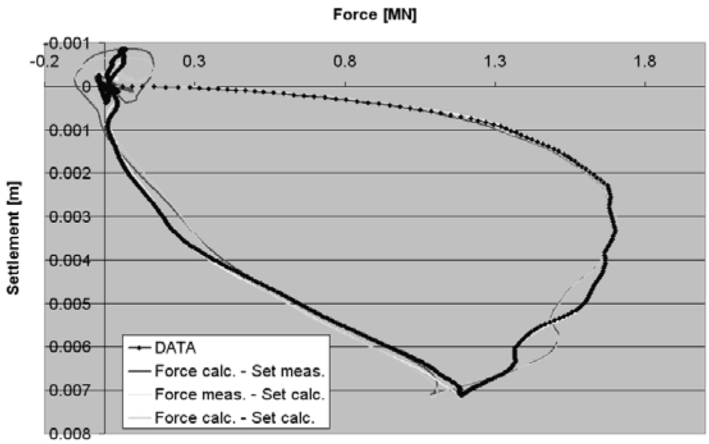

Figure IV-7 : Result of the optimisation : the load settlement curves

The imposition of the motion causes uncertainties in the evaluation of the force during the start of the unloading and at the end of the signal and the generation of the displacement based on the force signal [force meas. - set calc.] seems to be very successful and give a very good agreement with the original trace. The comparison of the measured signal with the double calculated signal [force calc.- set calc.] is the sign of a very good agreement but is not used to characterize the matching.

The time histories of each quantity is also a good way to confirm the quality of the matching procedure. Figure IV-2 and Figure IV-3 give an overview of these results for the signals of force and velocity. But it is also possible to check the settlement or acceleration agreements. The energy transferred to the pile (Enthru) can also be used as indicator of the quality of the matching procedure but instead of one sole curve as for the others quantities, the modelled enthru is function of the chosen function force and velocity (calculated or measured) used in its equation.

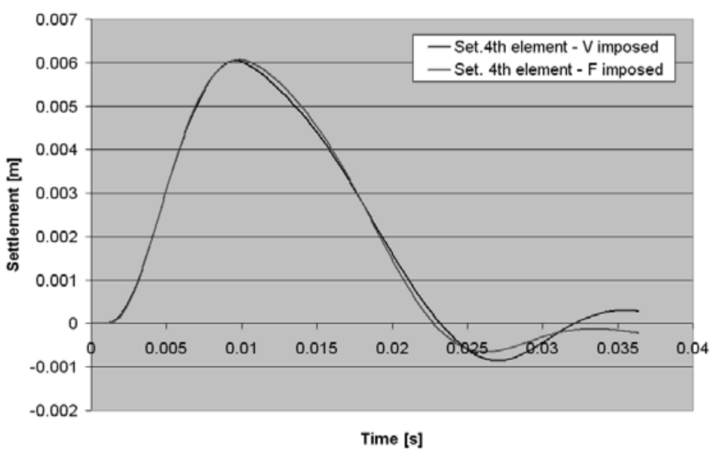

Figure IV-8 : Result of the optimisation : the settlement curves of the 4th pile element

The comparison of quantities at the pile head allows to compare the pile/soil response with the measured data. It is also possible to check the same quantities with depth along the pile. Since there is no possibilities of comparison with a real value, the comparisons only concern the signals generated by both types of signal imposition. The traces must be the most similar as possible.

2.4. Pile/soil system input

The pile soil system has to be introduced in order to give a first response. This description of the pile/soil system must be as relevant as possible in order to reduce the time needed to get an acceptable matching and to ensure a solution compatible with the pile/soil environment and logic with the quantity orders of magnitude: e.g. the soil parameters (ultimate resistance, initial stiffness, …) must be included in a well known range due to the knowledge of the soil constitution. The section dedicated to the parameters management in chapter 3 sorts the parameters in classes in function of their reliability and potential of variability. Essentially the soil parameters are concerned by the back-analysis process. The pile and test related parameters can be assessed with confidence.

The description of the subsoil is given by:

The shaft resistance parameters: maximum 5 layers with for each layer the depth z_i, the value of the ultimate shear strength $\tau_{ult,i}$, the initial tangent shear strength G_i, and the rheologic parameter J_i called the damping factor. A general value for the unloading modulus G_2/G_1 [-] is set for all the layers as the exponent of the viscous and rheologic ultimate terms fixed to 0.2.

The base resistance parameters: maximum 5 layers despite the fact that only the layers intersecting the cone of soil are taking into account. Each layer is characterized by the depth z_i, the value of the ultimate compression strength $\sigma_{ult,i}$, the initial modulus of elasticity E_i, and the damping factor J_i. As for the shaft, a ratio E_2/E_1 informing the unloading stiffness of all the layers is fixed. The Poisson ratio and the mass density are also required especially for the cone set-up.

Those soil parameters can be issued from several sources: geotechnical information from site, laboratory tests results, geophysical survey on field, experience of values by knowing the soil type or correlations between some of those quantities, are methods allowing to introduce a first pile/soil system description called the input of parameters.

Within this research, both sites of Sint-Katelijne-Waver (Boom clay) and Limelette (Bruxellian sand) have been extensively investigated with a large range of geotechnical tools and laboratory tests. The depths and the ultimate strengths for both shaft and base soil reactions are based on the electric cone penetration test (CPT-E) performed in the pile axis. The initial shear modulus and the initial modulus of elasticity are evaluated from the geophysical survey informing about the profile of wave propagation velocities V_p and V_s with depth. The typical soil parameters as Poisson's ratio and the mass density are based on the literature concerning the well documented soil types: Boom clay and Bruxellian sand. And the damping factors for shaft and base descriptions are fixed to 0.5 and 1 s/m$^{0.2}$ respectively, according to the literature.

The following figures summarize the data used for the analysis of the dynamic tests performed on the piles A7 of Sint-Katelijne-Waver and B8 of Limelette.

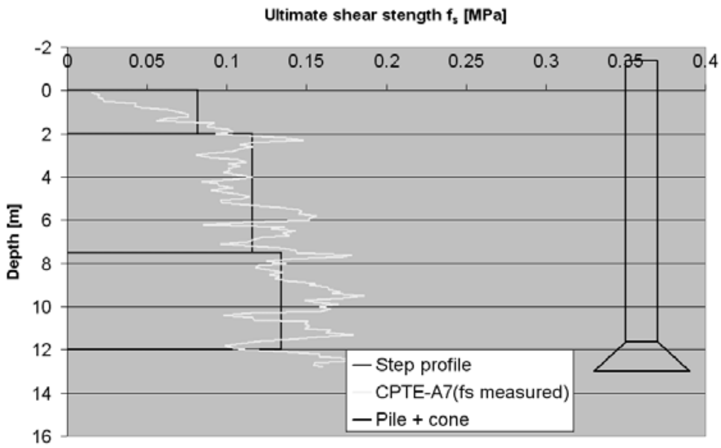

Figure IV-9 : Local friction strength from CPTE measurement and ultimate shear strength profile used in the back-analysis (SKW – pile A7)

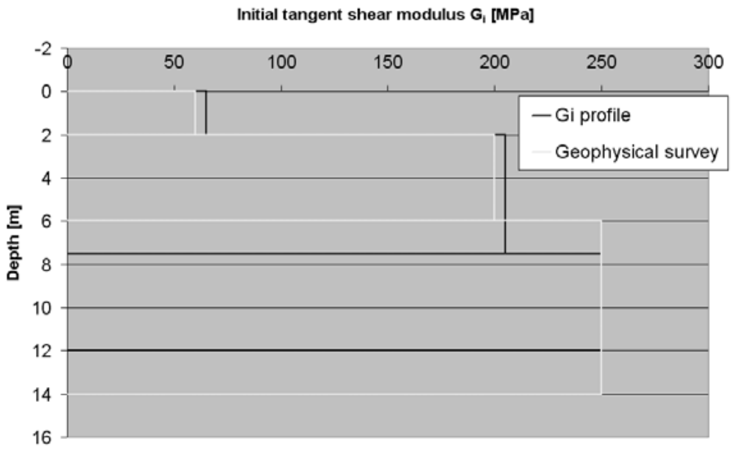

Figure IV-10 : Initial shear modulus from geophysical survey and initial shear modulus profile used in the back-analysis (SKW – pile A7)

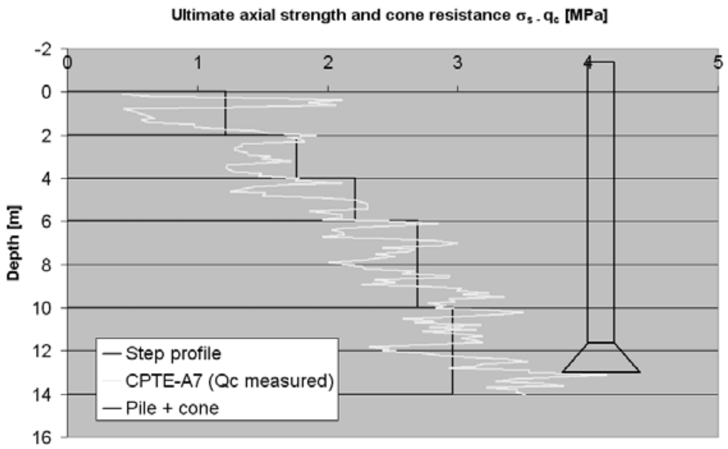

Figure IV-11 : Cone resistance from CPTE measurement and ultimate vertical stress profile used in the back-analysis (SKW – pile A7)

The ratio of modulus either for the shaft friction or the base resistance are both equal to 1 for this input definition and for both sites. the exponent N is also fixed according to the literature to 0.2 for the shaft viscous and ultimate soil resistance formulations and to 0.2 or 1 for the base viscous and ultimate soil resistance formulations.

The modulus of elasticity is based on the relationship linking the shear modulus to the elastic modulus and function of the Poisson ratio:

$$E = 2G \cdot (1 + \upsilon) \qquad \textbf{Equ. IV- 9}$$

For the concerned depths, the value of the initial modulus of elasticity in Sint-Katelijne-Waver is equal to 675 MPa and for Limelette to 800 MPa. The corresponding Poisson ratio are 0.35 and 0.45 respectively. The mass density of both materials is fixed to 2000 Kg/m³.

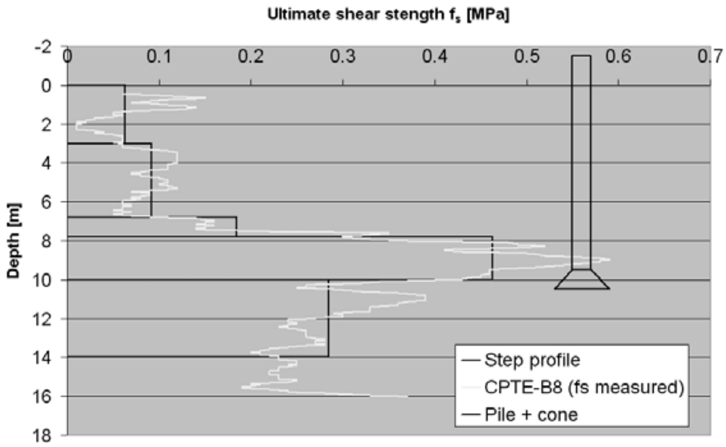

Figure IV-12 : Local friction strength from CPTE measurement and ultimate shear strength profile used in the back-analysis (initial) (Limelette – pile B8)

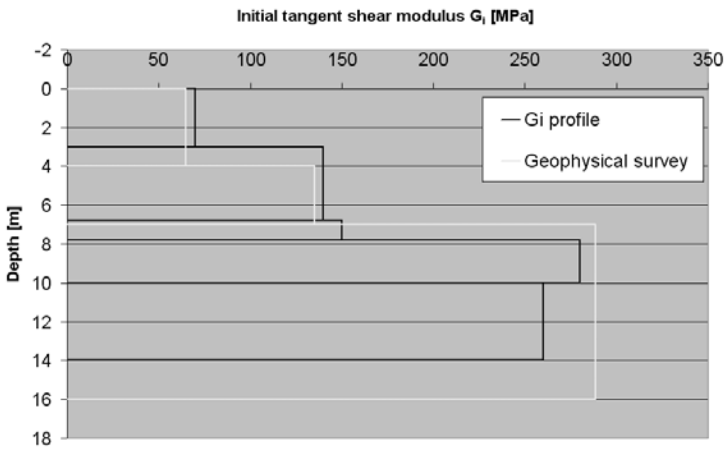

Figure IV-13 : Initial shear modulus from geophysical survey and initial shear modulus profile used in the back-analysis (initial) (Limelette – pile B8)

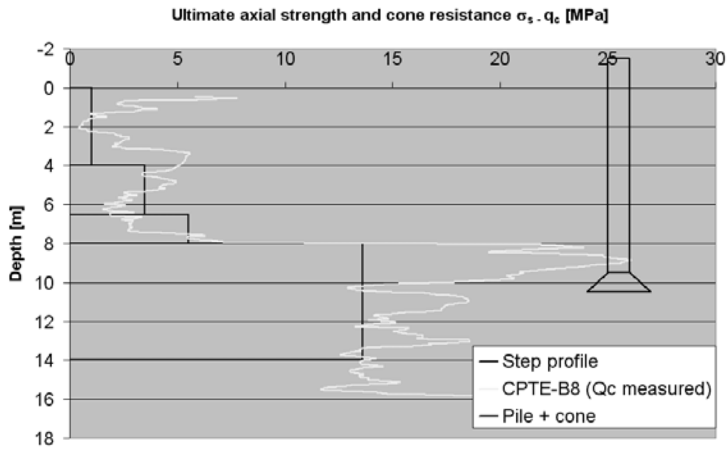

<u>Figure IV-14</u> : Cone resistance from CPTE measurement and ultimate axial stress (σ_v) profile used in the back-analysis (Limelette – pile B8)

This first description is used as start of the matching procedure. It gives the first point of the optimisation process. It seems to be logical to have the same point with all the analysis related to the same pile. It will be approached in a further section the question of the uniqueness which is directly linked to the relevancy of this point. These future developments highlight the importance to have a coherent input for the pile/soil characterization. The pile B9 of Limelette, located just next to the pile B8 uses the same input than the pile B8 as described here above.

3. Automatic optimisation system

3.1. Requirement

The condition to perform the back analysis are as follows:

- the signals are of good quality;
- the pile geometry is well known and well described;
- the pile is well shaped and its integrity reliable;
- the wave propagation velocity inside of the pile material is well evaluated;
- the pile/soil model is correctly built (choice of the fundamentals relationships, of the pile discretization and the numerical procedure).

With these assessments , the back-analysis can be launched with the modification of the resistance and the rheologic parameters in order to fulfil the agreement between measured and calculated curves.

In some previous procedures, this operation was conducted manually and concerned only the values of the ultimate strengths. All the other parameters (rheologic, thickness of the soil layers, initial shear modulus and modulus of elasticity) were not modified directly. Their changes were not supposed to be influential. If it is true that the ultimate soil resistance is a very powerful class of parameters in the matching procedure, it will be shown that the others parameters have their own influence and there is real danger to forbid them to be variable during the back-analysis. However, the number of parameters is directly function of the difficulty to find out an acceptable solution. 2 to 5 layers of soil x 4 unknowns (τ_{ult}, z, J, G) for the shaft reaction plus 1 or 2 layers of soil x 4 unknowns (σ_{ult}, z, J, E) for the base reaction plus the unloading moduli (2) give a total of 14 to 30 unknowns to be optimised with the only guide of two couples of curves to fit in between.

This set of n parameters **p**={p_i} and their respective range of variability gives a response of the pile/soil model for each combination of them. This response is evaluated with the criterion D_p as:

$$D_p = f(p_1, p_2, ..., p_i, ..., p_n)$$ **Equ. IV- 10**

This function is a surface of dimension n (according to the number of parameters to be optimised) in the system of dimension n+1 (Figure IV-15). The purpose is to find the minimum of this surface and to respect the domain of validity of each parameter and some physical constraints.

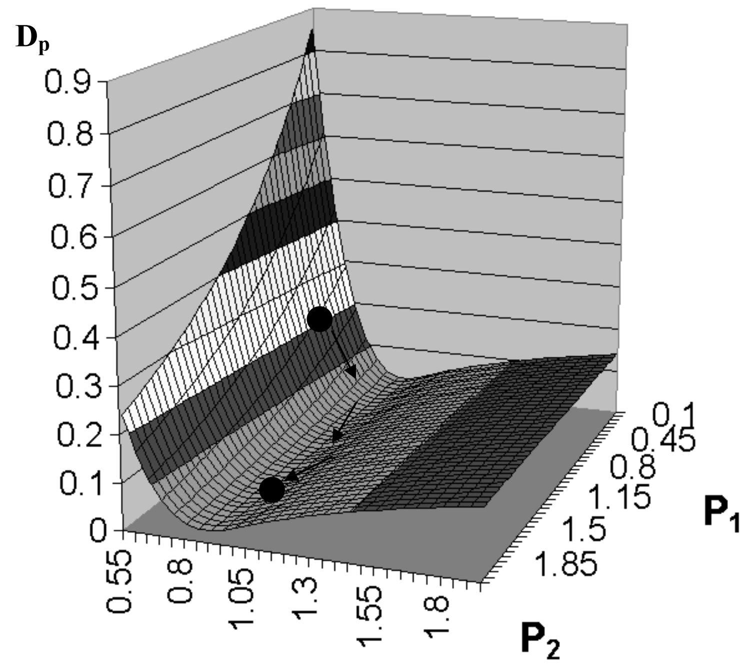

Figure IV-15 : Surface of the matching quality factor function of 2 parameters (p_1 & p_2)

The modification of one parameter modifies the influence of the other parameters on the pile/soil system response. The relative influence of each parameters is given by the partial derivation of the function with respect to the chosen parameter. That can be translated as the slope of the surface in the direction of the parameter axis. If the operator modifies one of the parameter manually, all the others are influenced in function of the distance travelled on the surface. There is a need to investigate all the parameters at the same time and to chose the best way to reach the solution in function of the variability of each parameters. But this operation is not achievable without an automatic operation managing all the parameters or allowing to do it for a given number of them.

Moreover, the optimisation requires a large number of iterations and small modifications of parameters in order to find a stable and best final characterization of the pile/soil system. Indeed, a large modification generally prevents to stabilize the process and to refine the solution. This high number of iteration requires also the setting up of an automatic procedure.

Finally, the need to study the sensitivity of the pile/soil response to particular modifications of some parameters and the necessity to ensure an impartial process imposes also this approach.

3.2. Literature

Several authors and methods use an optimisation process based on a self made algorithm or an existing method developed in the applied mathematics domain.

CAPWAP® uses an iterative algorithm based on the modification of resistance parameter in order to minimize the deviation given in Equ. IV- 4. The signal is optimised either on the force or on the upward wave signal (imposition of the velocity or downward wave as boundary input, respectively).

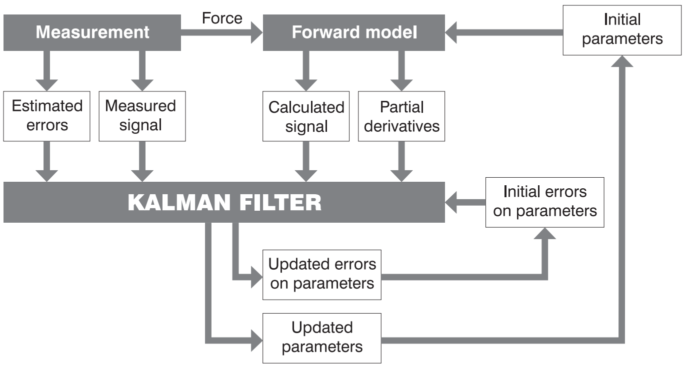

Figure IV-16 : TNOWAVE algorithm of matching (after Van Foeken et al., 1998)

TNOWAVE® uses a pile soil response from the imposed boundary condition based on its typical pile/soil model (chapter 1). It is called the "forward model" (Van Foeken et al (1998) & Courage & et al (1992). An algorithm called the Kalman fiter (Kalman (1960); Hendriks et al. (1990) and Courage et al. (1990)) is used in order to estimate the unknown parameters values and their a posteriori covariances so that a good agreement is found between the measured data and the forward model response. The a posteriori covariances inform about the reliability of the values found. With the impact signal and initial parameters description, the forward model computes the pile/soil response. This response, together with the measured one is supplied to the Kalman filter. Based on the difference between both signals and the partial derivatives of the responses with respect to the parameters (using a perturbation method) and the covariance of the measurements, the parameters and the chosen model, the Kalman algorithm calculates a gain to update the parameters and their covariance. The procedure is repeated until a convergence criterion is met. In dynamic signal matching, the match is done on the upward travelling wave.

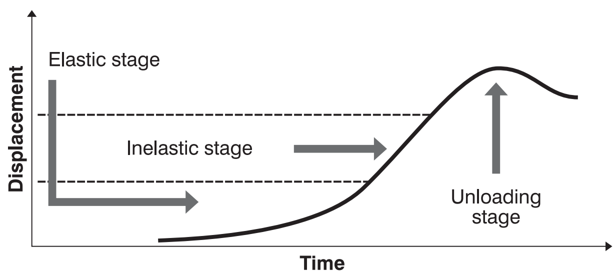

Figure IV-17 : Typical displacement-time history curve (after El Naggar et al., 1998)

El Naggar and Baldinelli (1998) describe an iterative automatic matching technique focused on the statnamic load test optimisation based on the decomposition and the fitting of the displacement signal into 4 distinct phases. The method uses the pile/soil model of El Naggar and Novak (1994) describing the response of pile under dynamic loading (see chapter 2). This model and the initial set of parameters calculate a response of the pile to the statnamic load introduced as boundary condition. The computed displacement response is compared with the measured one. Each one is fitted with a set of polynomial functions and connected to a few number of parameters significant in this part of the curve and adjusted with priority:

- The elastic stage of the displacement time history is fairly linear, is governed by the stiffness of the soil medium and derived from the elastic properties such as shear modulus and mass density. The function modelling this phase is a linear function;
- The inelastic stage is faily non-linear due to the pile response at higher load level. The end of this stage is associated to the time of maximum applied load when the unloading phase begins. This phase is governed by the soil resistance parameters and depend of the chosen rheologic model. A quadratic function represents the pile response during this stage.
- The unloading phase is also non-linear and divided in two sections. The first is between the maximum load instant and the peak of displacement. This section is modelled by a quadratic function, and the next phase starts at the peak displacement and ends at the moment the displacement becomes constant around its permanent value. This section is also modelled by a quadratic function. The ultimate soil resistance, the shear modulus at the base and the eventual post peak soil resistance govern the unloading stage.

After fitting the stages of the displacement signals, measured and computed, with the appropriate functions, the convergence criterion is calculated (Equ. IV- 5). The constant of the regression analysis and the area of each curve are used to adjust the soil parameters in each iteration. After fulfilment of the convergence, the parameters, which resulted in the best fit, are used to model the pile response to any solicitation.

Berzi (1994, 1996 & 1999) developed an efficient secant-method based algorithm for solving non-linear least squares problem presenting a good stability and convergence properties even with large number of unknowns. He applies this resolution technique to the dynamic pile/soil interactive system. The method is based on the willingness to fit a structured mathematical model to available data expressed by a surface in the n +1 dimension system composed by the n parameters of the structured mathematical model. He transforms the parameter identification problem in a non-linear least squares problem in which the solution is given for parameters values providing a minimal deviation between observed and simulated system response and the normalized error. His algorithm is based on the works of Wolfe (1959) with an improvement of the convergence with a special selection of the search direction. The non linear system is function of the pile/soil interaction system through the definition of the gap between the observed system and the simulated response. The latter is function of the system definition and the parameters values:

If
- $\mathbf{p} =[p_1, p_2, \ldots, p_n]$ the n parameters of the system (1, …,n);
- $\mathbf{p^0}$ = the initial set of values for $\mathbf{p}$;
- $D(\mathbf{p})$ = the gap (normalized) between the observed and simulated pile/soil responses;
- $r_j(\mathbf{p})$ = the partial area between two corresponding couples of points of the observed and simulated pile/soil response (1 to m) (Figure IV-4

- the observed and simulated pile/soil response are composed of m points;
- **r(p)** = the vector of r_j**(p)**.

then, the parameter identification problem can be formulated as a system of non linear equations:

$$r(p) = 0 \quad r : \Re^n \to \Re^m \quad m \geq n$$ **Equ. IV- 11**

The basic idea is to replace the non linear system of Equ. IV- 10 by a linear problem. It consists of linear interpolations through n+1 solutions [$\mathbf{p^i}$, $\mathbf{r(p^i)}$] (I=0, …, n).

The management and the choice of the successive [$\mathbf{p^i}$, $\mathbf{r(p^i)}$] represents the algorithm leading to the solution **p*** minimizing **r(p)**.

All these methods propose good ideas that were integrated partially or not in the development of the following optimisation method.

The method proposed by El Naggar and Baldinelli (1998) seems to be very attractive for statnamic tests because of the high number of data available for the different stages described. It is more difficult to apply this procedure to dynamic tests due to the quick loading and the small number of points available before the last stage, namely the unloading phase.

The methods used in CAPWAP® and TNOWAVE® seem to be very attractive but look like a black box procedure with a few details on the evaluation of the parameters gain at each step of the procedure. Consequently, the need of a global and automatic optimisation procedure remains like the need to develop it.

Finally the Berzi method is well described and defines the problem of the parameter identification with back analysis in a theoretical way. But the method looks like too mathematical. Moreover, the purpose is also to evaluate the path used by each parameter before reaching the optimal position in the R^n system and to integrate the procedure in a global program based on a explicit method of resolution and not a method based on matrix resolution. But the system should be developed and compared with other methods of optimisation.

3.3. Algorithm

The method developed in this research is inspired of a process used to analyse the sensitivity of the neighbourhood of the optimal solution in order to evaluate the potential local minimum and to evaluate the influence of variability of each parameter around the found solution. As explained in section 3.2, Berzi developed this approach in 1996.

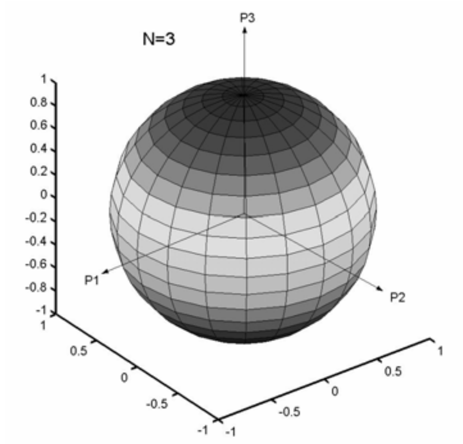

Figure IV-18 : Analysis of the neighbourhood of the optimal solution

The neighbourhood of the optimal solution **p*** is systematically explored. With 3 parameters, if the solution **p*** is given, the systematic exploration around this point is a sphere of radius Δ (Figure IV-18). The exploration is made randomly in the parameters space R^n. The pile/soil response is evaluated with D**(p)** determined for each combination of parameter values and associated to the vector **p**. Generally, the point environment is investigated with successive and decreasing values of Δ. The collection of points and the corresponding values of D**(p)** characterize the quality of the interpretation and the effects this interpretation on the simulation of the static load settlement curve.

The principle is the following:

Each parameter p_i is modified such as $p_i = p_i^* + \Delta p_i$ **Equ. IV- 12**

Where Δp_i is the variation added to the parameters p_i^*. Δp_i can be positive or negative.

The condition allowing to quantify this variation for each parameter of **(p)** is the radius of the n-ball in the parameters space R^n:

$$\Delta = \sqrt{\sum_{i=1}^{n}\left(\frac{\Delta p_i}{p_i^*}\right)^2} = Const.$$ **Equ. IV- 13**

Δ is limited to the range [0,1] because the parameters values can not be negative due to the physical meaning of the parameters, so that the ratio $\frac{\Delta p_i}{p_i^*}$ must be lower than 1.

Determining randomly the combinations of the vector Δ**p** but respecting the rule of Equ. IV- 13 allows to know the effect of a determined variation of the parameters on the quality criterion D**(p)** and possibly on the simulated load-settlement curve. A large number of these vectors are generated and the result of D**(p)** is sorted as a function of the radius Δ used and as a function of an unequivocal quantity evolving with the variation of parameters e.g. the ultimate soil resistance, … This method is called the *multidimensional parameter perturbation sensitivity analysis* (Berzi, 1996).

The use of this technique in the optimisation process is based on the extensive random study around a particular value of **p** and the systematic evaluation of D**(p)**. Instead of analysing the variation of D**(p)** around $\mathbf{p}^*$ optimal, the minimum of D**(p)** is sought around the vector **p** which is not the optimal solution.

If the pile/soil system is characterized by the vector $\mathbf{p^0}$ defined by the input (page 8) and the corresponding D($\mathbf{p^0}$), the value of the quality criterion for this configuration, a systematic study of its neighbourhood for a given radius Δ and k combinations of **p** according to Equ. IV- 13 can evaluate each $\mathbf{D(p^i)}$ and find the best vector **p'** amongst all the tested combinations of **p** such as:

$$D(p') \leq D(p^i) \quad (i = 0...k)$$ **Equ. IV- 14**

When the best solution is found for the random set of combination of **p** around $\mathbf{p^0}$, the new set of parameters characterizing the pile/soil interaction system is changed from $\mathbf{p^0}$ to **p'**:

$$p^0 = p'$$ **Equ. IV- 15**

And the set process is started again until reaching of the minimum minimorum. This method is illustrated by Figure IV-19 for two parameters and resumed by the algorithm Figure IV-21.

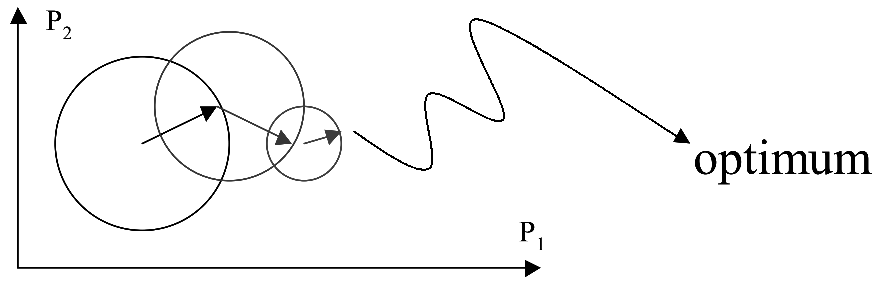

Figure IV-19 : Schematic procedure of optimisation for 2 parameters

There are conditions for the evaluation of the number of the combinations k tested around $\mathbf{p^0}$, for the definition of the radius Δ, for the end of process conditions and for the evaluation of the optimum value of $\mathbf{D(p^i)}$ in each loop of the optimisation process. All these steps are described in next sections.

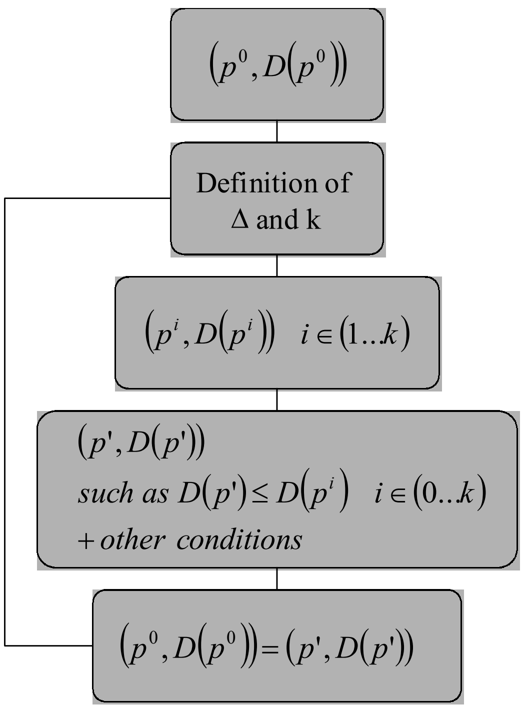

Figure IV-20 : Algorithm of the sensitive method of optimisation

This method have the following advantages:

- The step by step way of resolution allows a control on the parameters inside of their range but also in comparison with the environment and the other parameters;

- All the parameters evolve at the same time. A procedure that optimised the parameters one by one was also tested during this research, but the correlations between parameters influenced the quality criterion. The simultaneous upgrade of two parameters is often more benefit than the sole and consecutive modification of the same parameters;

- This method, open and explicit, allows to store the evolution of the optimisation in order to check the variation of each parameters. The relative weight of each one can be assessed in function of the optimisation progress. Moreover, the path followed is known and attests of an evolution or an erratic progression.

There is also disadvantages:

- The random evaluation of a large number of combinations can be a waste of time and does not represent an advanced methodology;
- There is no certainty that the best combination is not a local minimum

These disadvantages must be taken into account by the setting up of methods improving the choice of the best combination by testing the combination with respect to the a priori knowledge of the pile/soil system, by checking out the path followed in order to identify a trend in the parameters evolution and by rendering more reliable the method of construction of the combinations.

Two methods were tested in order to carry out this algorithm. The first one is rigid and the second is more open. They differ by the choice of k, Δ, and the choice of the of **p'**.

The first approach imposes the values of k and the schedule of Δ investigated. That means the algorithm follows a determined sequence of radius. The optimisation starts always with the larger radius in order to progress as fast as possible; this radius is progressively reduced until reaching the end of the sequence.

The schedule of Δ allows to test the same radius several times before changing and reducing it. For each radius, a determined number of combinations is tested and the set of parameters giving the best result amongst all these combinations (according to the criterion of quality) is chosen as new reference for the following steps. The procedure ends when the last radius envisaged is tested. This method generates a lot of non-used evaluations for one sole modification in each step. But this choice of the best combination can be made with statistical methods because the large number of succeeding combinations allows it. This method lasts also longer than the next one.

The second approach is more sensitive. A start radius is determined, generally rather large, and for each combination $\mathbf{p}^{\mathbf{i}}$ tested, a comparison is made with the previous criterion of quality (D(p)). If all the recommendations testable agree, the modification is performed immediately and the new position of reference in the n-system becomes this new found combination of **p**. The radius Δ does not change until a particular criterion is fulfilled: if a certain number of combinations is attempted without improvement of D(p), the radius is automatically reduced. The optimisation procedure ends when the determined lower radius is reached and no improvement have been noted since a fixed number of trials. This method is faster and generates more intermediate changes, but only small number of tests can be applied on each particular successful combination to check its validity. For each method, it is possible to choose the parameters to be optimised. A list is composed before the start of the procedure. This allows to refine some parameters less influent when the best solution is almost reached.

3.4. Uniqueness of the back-analysis response

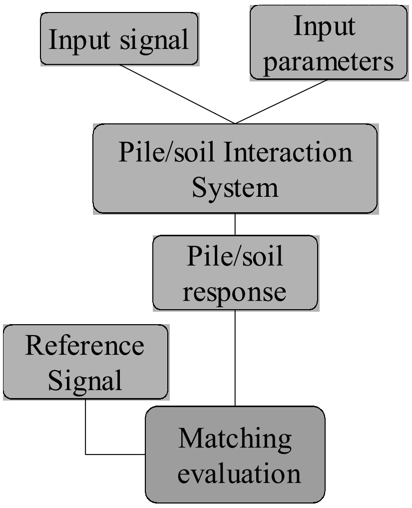

Figure IV-21 : Scheme of the back-analysis process

Since the pile/soil interaction characteristics are back-calculated from the results of dynamic loading test in order to simulate the load-settlement relationship, the reliability of the latter depends on both the quality of the measured data and the quality of the analysis. The quality of the data has already been discussed earlier (chapter 3). The precision inherent to the analysis is function of the validity of the pile/soil interaction model chosen to represent the real system and of the method used for the "signal matching" and the back-analysis. It is known that the solution of the inverse problem is never unique due to the measurement noise and modelling inaccuracies (Berzi, 1996). Nevertheless, this problem is linked to the hypothesis assessed and not to the system supposed to perform the analysis.

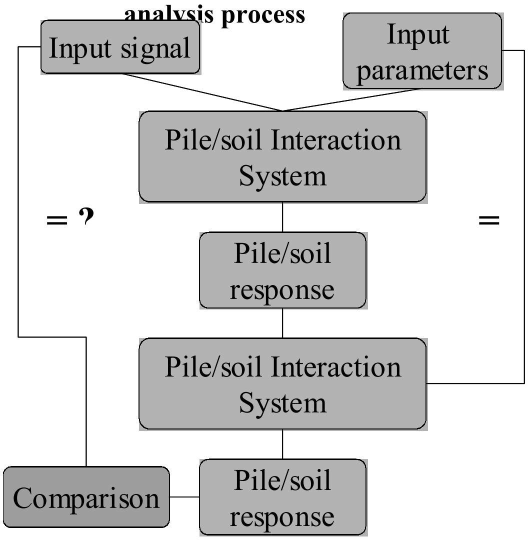

Figure IV-22 : Scheme of verification of the system (#1)

It is proposed in this section to briefly validate the system and to check the reliability of the back-analysis process (Figure IV-21) with a double crossed analysis of a real test (Figure IV-22 & Figure IV-24):

1. The test consists to impose the input signal and the input parameters to the system, and to re-inject the pile/soil response obtained in the pile/soil system to compare the result with the first input signal. If the system is reliable, both signals agree perfectly (Figure IV-22). A signal of force measured on field during the Limelette campaign is used as first input signal (B9-013).

Figure IV-23 shows both signals of forces: the imposed and the computed ones. The agreement between both curves is perfect. This test validates the system and allows to use crossing signals to characterize the matching process.

2. A second test is based on the back-analysis itself. Is the process repeatable? Is the solution or the area in the n-space of parameters representing the unique solution? In order to test this assumption, the algorithm described in Figure IV-24 is followed. A force signal is injected as input in a given pile/soil system characterized by the input parameters set #I. The pile response is re-injected in a second pile/system from where the parameters are back-analysed in order to have a perfect agreement between the first input signal and the last pile/soil response. The input characterisation of the second pile/soil system (#II) is set completely different from the solution in order to check a different path. The purpose is to compare the initial input I with the result of the back analysis (Figure IV-24).

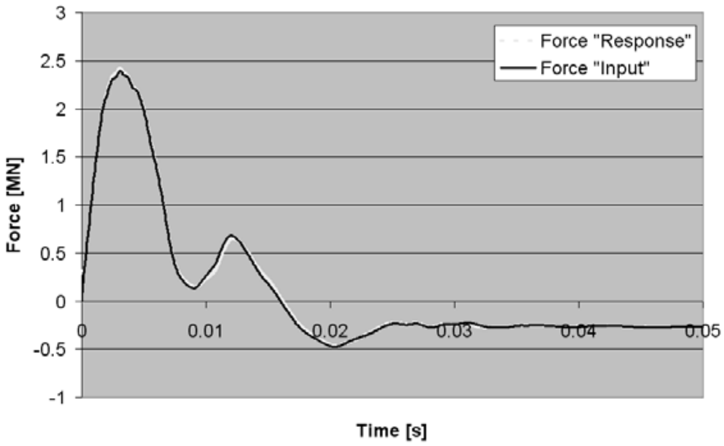

Figure IV-23 : Validation of the system : comparison of forces measured and calculated

Three optimisations with three types of input characterisation are successively performed. the reference input is displayed on Figure IV-27 to Figure IV-30 and Table IV-1 with the label "Reference" (from the Limelette measurements previously used (B9-013):

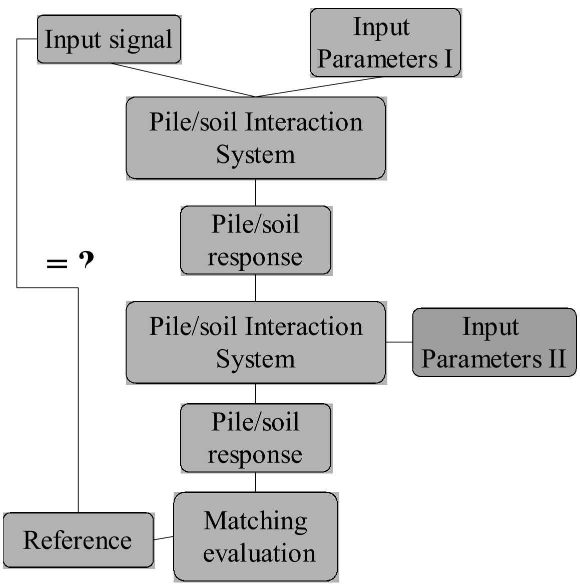

Figure IV-24 : Scheme of verification of the back analysis tool (#2)

- "Optim1" is proposed with a profile of ultimate shear strength constant with depth and equal to 0.15 MPa. The ultimate base resistance is set to 13 MPa;
- "Optim2" is proposed with a shaft inverse profile (the maximum resistance close to the pile top, and the weakest to the pile bottom). the ultimate base resistance is set inferior to the reference one (about 1.4 MPa);
- "Optim 3" has simply the same ultimate resistance profiles (base and shaft) than the reference one but doubled.

The depth, stiffness and damping factor profiles do not have been modified. The ultimate resistance parameters have the most significant influence on the matching process and too much changes bring a misunderstanding of the results.

After optimisation, the quality criteria are very low: D(p) less than 0.16 % for optim1, 0.73% for optim2 and 0.26 % for optim3 for a study duration of about 20L/c. Moreover, the load-settlement curves (Figure IV-25) and the acceleration and velocity traces are almost superimposed (Figure IV-26). In a strict matching aspect, the process is successful and the back analysis gives theoretically the same pile/soil characterization characterizing the pile/soil interaction. It remains to compare the parameters profiles to check the most important: the reliability of the process in the parameters determination.

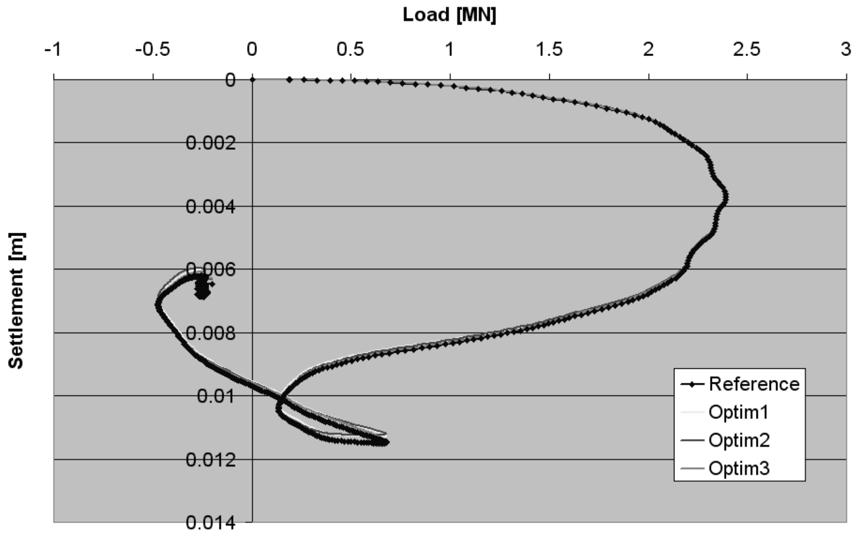

Figure IV-25 : Validation of the back-analysis procedure – comparison of the measured and calculated load settlement curves

The acceleration traces (Figure IV-26) present a small difference, especially the optim2 case, compared to the reference. Globally the matching is very good, but there is a slight perturbation between the instants 0.007 and 0.023 s. Since the problem is almost concentred on the optim2 case, this could be a sign of quality of the back-analysis process. The acceleration traces remain very difficult to match. However the quality of the matching is particularly remarkable because of the length of the study (more than 50 ms), due to very low value of D(p) for all attempts and also due to the almost perfect agreement between calculated and measured signals for all quantities (force, displacement, velocity and acceleration).

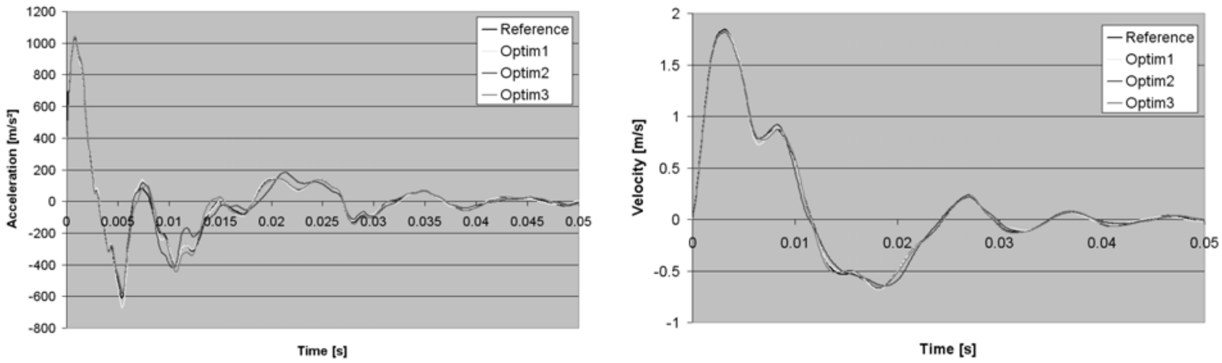

<u>Figure IV-26</u> : Validation of the back-analysis procedure – comparison of the measured and calculated acceleration and velocity curves

The velocity traces are also well modelled. The trace related to the 2nd optimisation is still the worst.

<u>Figure IV-28</u> to <u>Figure IV-32</u> display the result of the back-analysis in terms of parameter profiles after the optimisation stages. <u>Figure IV-28</u> and <u>Figure IV-29</u> present the ultimate and the maximum reached static shear stresses obtained. <u>Figure IV-31</u> shows the integration of the soil reaction along the pile shaft plus the base static soil reaction. Finally <u>Figure IV-30</u> gives the detail of the reached maximum vertical stress at pile base for each optimisation process and the ultimate value obtained and <u>Figure IV-32</u> gives the ratio in % of the maximum shaft friction reaction and total soil reaction with the corresponding reference.

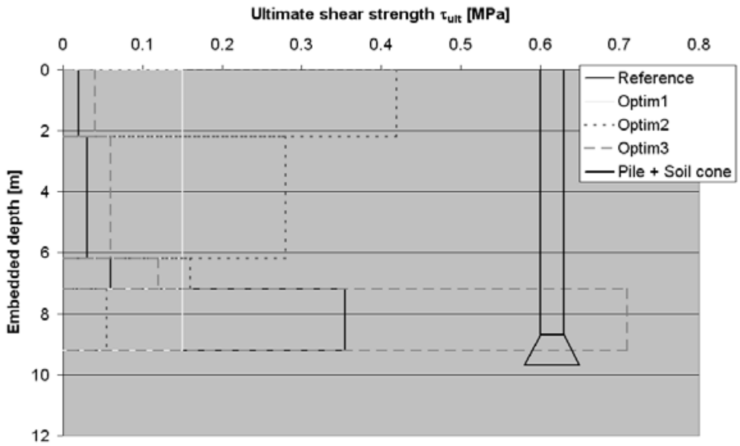

<u>Figure IV-27</u> : Ultimate shear strength initial profiles

The profiles are displayed with reference to a Prefab pile from Limelette. The only embedded part of the pile (without excavation) is represented.

The profiles of ultimate shear resistances (<u>Figure IV-28</u>) present a mutual general profile and variable discrete values. Taking into account that the input profiles were very well differentiated, the global shape of each result present an evident similarity with the reference, which is an extremely good result. The soil profile remains unchanged (a weaker soil layer along almost the all pile and a stronger layer close to the base: this profile is noted “reference” on <u>Figure IV-28</u>) and can be determined from a dynamic load test with the back analysis process. On the other hand, the net values are rather variable:

the ultimate shear resistances of the strongest soil layer vary from 0.29 to 0.46 MPa. The thickness of the layers is also quite different. The thicker the strongest layer, the less resistant the corresponding ultimate shear stress.

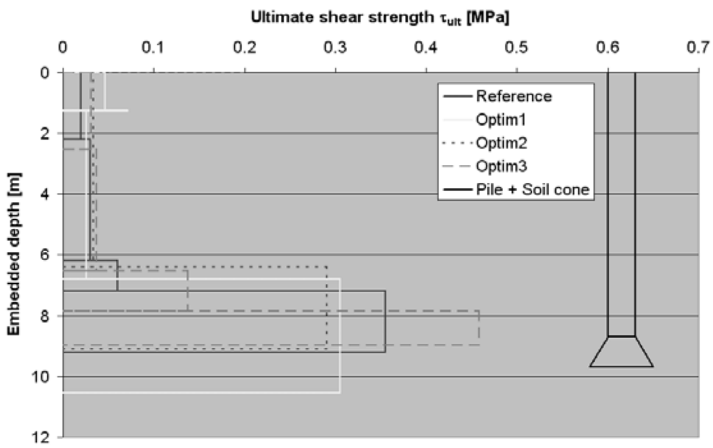

Figure IV-28 : Ultimate shear strength profiles

Most of the soil layers, especially along the pile shaft, are fully mobilized during the pile loading. But this is not the case for the base resistance and the strongest soil layer because the displacement imposed is not sufficient. Figure IV-29 presents the maximum shear stress reached for each pile element during optimisation. As expected, the weakest zone completely mobilizes the soil resistance and the last layer presents smaller values of soil reaction than their ultimate corresponding. However, a difference remains between the optimisations, what is relatively problematic within the framework of the static load-settlement relationship (max stresses reached vary from 0.23 to 0.42 MPa) even if the corresponding thickness seems to be inversely correlated to this variation.

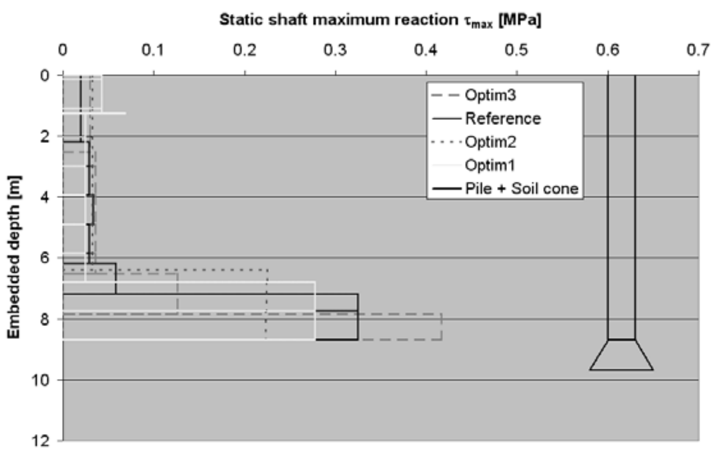

Figure IV-29 : Maximum shaft friction τ_{max} profiles

Figure IV-30 present the maximum reached vertical stress at pile base and the values of the ultimate vertical stress obtained with the back-analysis. optim1 and optim3, which have started from a higher value than the reference one (for both ultimate and maximum values) are very close to the reference result. On the other hand, the 2nd optimisation is inferior for both maximum and ultimate values. This corresponds to the worst quality of this matching process seen on the signals traces (Figure IV-26).

Moreover, the two remaining trials have an ultimate base resistance superior but not excessively. These observations may indicate that the base ultimate resistance must be set superior to the estimated one in order to have a correct evaluation and that the ultimate values are of importance but the max values reached during the test are more important. This is confirmed by Figure IV-31.

	Ultimate static base resistance σ_{ult} [MPa]
Reference	5
Optim 1	13
Optim 2	1.4
Optim 3	10

Table IV-1 : Ultimate base strength values

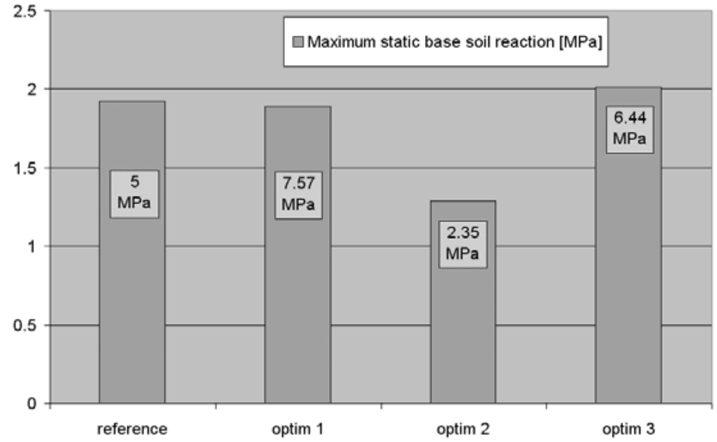

Figure IV-30 : Maximum vertical static stress

Since a balance may exist between the thickness and the maximum shear stress reached for each optimisation, it seems to be evident to integrate the reached stresses along the pile shaft plus the base mobilization and to compare the four results with respect to depth (Figure IV-31). The comparison and the results are remarkable. The curves present the same behaviour, quickly modelled by an addition of two straight lines defining two types of soils. The depth of change is also conserved (about 7 m).

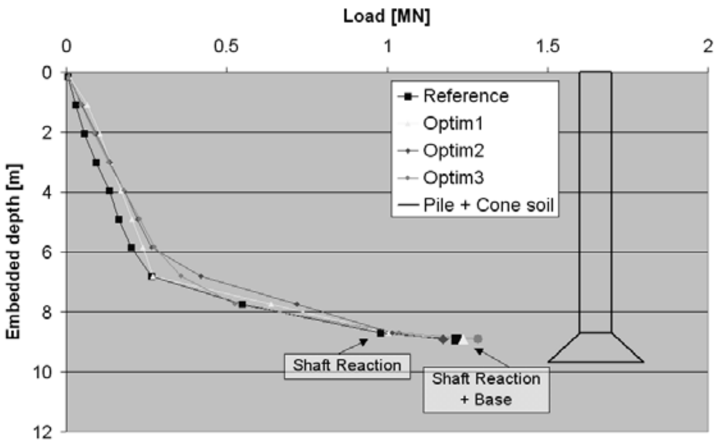

Figure IV-31 : Cumulated load along shaft + base

These results confirm the fact that the most important in the modelling and the back calculation is not the ultimate stress, neither their maximum reached stress but the all resistance in function of the depth along and beneath the pile. Only the profile of the second optimisation seems to be slightly different by a start of the strong soil layer a few earlier than the other cases. This is probably to compensate the lack of resistance coming from the base at the start of the optimisation. This fact highlights the importance of the quality of the initial Input in value and profile.

This result is extremely good. The final results of the back-analysis evaluate the same soil reaction along the pile depth even if the input characterizations are rather different. Figure IV-32 presents the ratio of loads for both shaft and total details with the corresponding reference. The results are very close to the reference one. Only the influence of the weakest base of the 2nd trial causes a small difference.

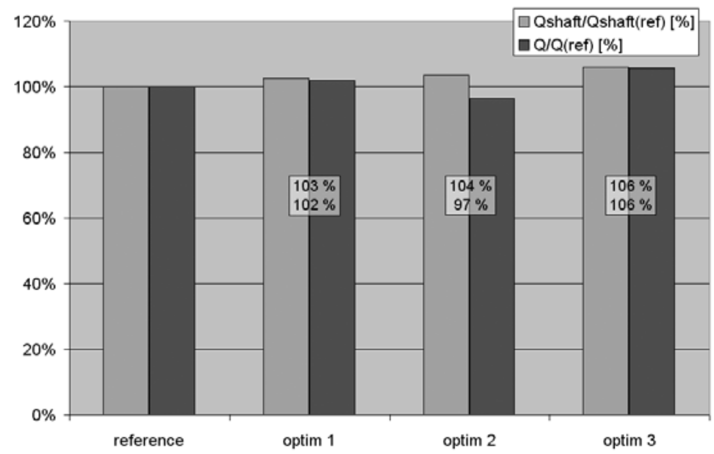

Figure IV-32 : Evaluation of the shaft and total soil reaction compared to the reference (in %)

Finally, Figure IV-33 displays the simulations of the static load-settlement curves until the depth of the maximum settlement reached during the test. It can be seen that optim1 is almost perfectly superimposed to the reference simulation and optim3 is slightly overestimated (but not significantly). The most pronounced difference is seen with the 2nd optimisation due to the weakest base soil reaction. For the others, the curves are remarkably grouped.

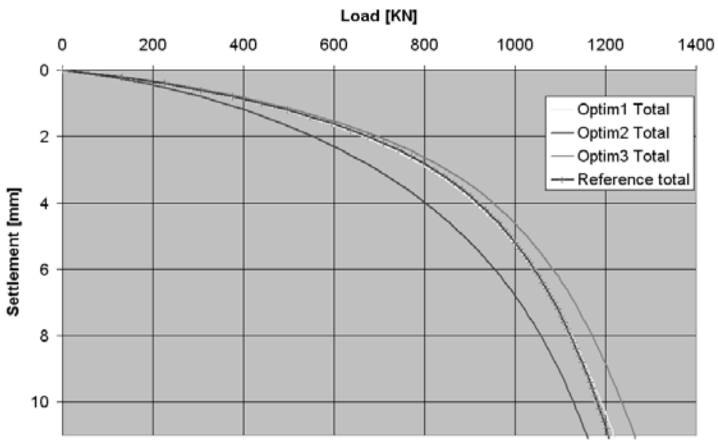

Figure IV-33 : Simulated static load-settlement curves

This result allows one to conclude that the back-analysis process is globally reliable in the total soil reaction mobilized point of view. The ultimate resistance evaluated must be taken into account with interest in order to assess of the global evolution of the profile but there is a balance occurring between the thickness of each layer, their ultimate resistance and the maximum reached resistance in order to balance the total mobilized reaction that seems correspond to a invariant amongst the results of the three back-analysis. Moreover, the strict result of the matching procedure is a needed condition to have a good back-analysis process but not a sufficient condition.

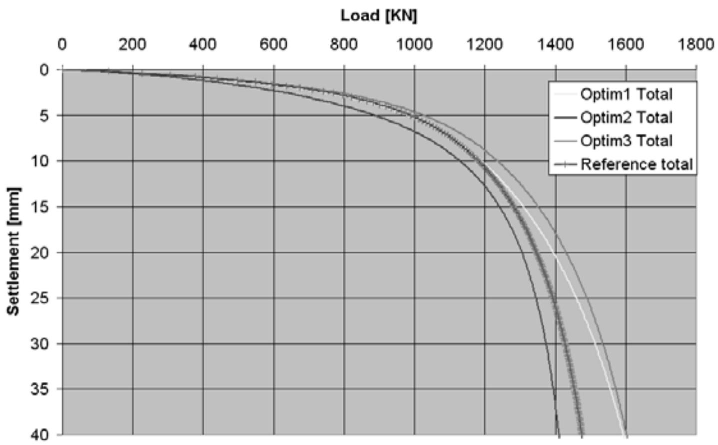

Figure IV-34 : Simulated static load-settlement curves

Another test is needed to confirm the good result of a successful matching between dynamic curves. For example the profile obtained must be correlated with an external source of information (geotechnical, …).Finally the simulated curves are valid for the only settlement mobilized during the dynamic test. If larger settlements are taking into account, the mobilization of the base is completely estimated and not checked out by comparison with measured data. That causes a more spread out result (Figure IV-34).

4. Sensitivity of the result to a parameter variation

4.1. Sensitivity analysis and representation of the matching quality

It is known that the solution of the inverse problem is never unique due to the measurement noise and modelling inaccuracies (Berzi, 1996). It just has been observed in the previous section that the back-calculated values of the parameters can vary following a certain combination of each other allowing to obtain a given matching quality. Instead of having discrete and inalienable parameters values from signal matching, the optimisation result is more a combination of the whole parameters representing a cloud within the n-space of parameters.

Some of the parameters are more influential than others. The same percentage of variation does not influence the signal matching result with the same magnitude. That determines the shape of the cloud in the n-space. The size of this cloud is determined by the required precision in the matching procedure. Finally the precision required for the parameters to ensure a certain accuracy in the matching procedure influences subsequently the simulation of the static loading procedure. Consequently, it is important to characterize this variation in order to qualify the influence of each parameter and the influence of each category of parameters on the matching process and on the simulation of the static load-settlement curve.

The method used to investigate the influence of the variability of each parameter or its sensitivity is based on the *multidimensional parameter perturbation sensitivity analysis* (Berzi, 1996) (see section 3.3). The point of which the neighbourhood is investigated remains constant and is the optimal solution **p***. The exploration is made randomly in the n-space R^n only defined by the radius Δ.

The modifications of the parameters p_i follow the same process than in Equ. IV- 13 & Equ. IV- 14.

The pile/soil response is evaluated with D**(p)** and each combination of parameter values $\mathbf{p_i}$ is associated with the corresponding D(p).

Δ	N
0.8	600
0.7	600
0.6	500
0.5	500
0.4	400
0.3	400
0.2	300
0.1	200
0.05	100

Table IV-2 : Sensitivity analysis

Generally, the point environment is investigated with successive and decreasing values of Δ. The values of Δ and the number of generated vectors are selected so that the size of the statistical sample is suitable for analysis. Table IV-2 summarises the advised size of the samples needed with respect to the radius Δ.

The results can be expressed in several forms. The classical representation of the sensitivity analysis is given by the variation of D(p) in function of the variation of one parameter.

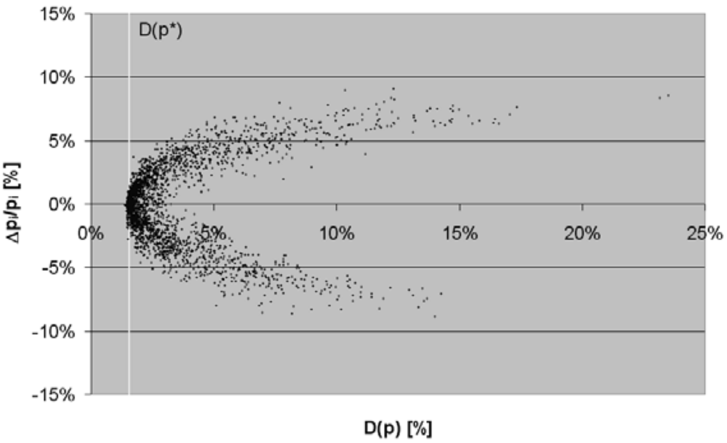

Figure IV-35 : Variation of D(p) vs. the variation of an influent parameter

Figure IV-35 to Figure IV-37 represent the variation of the matching quality factor D(p) with respect to the imposed variation of one parameter ($\frac{\Delta p}{p}$).

The analysis presented in the following figures is based on the result of the optimisation of the 13th blow of the pile B9 of Limelette. The result of the optimisation give a result of D(p) of about 1.57% (the minimum value is marked with a vertical line on the figures). The sensitivity analysis has been performed using the radius Δ of 5, 10, 25, 50, 65, 80 and 90 %. The analysis was applied on 25 parameters and based on a total of 2900 generated points. A lot of points are located in the close vicinity of the matching optimum: 273 combinations (9.4%) give a better matching and more than 40% of the combinations represent a matching inferior to 2%.

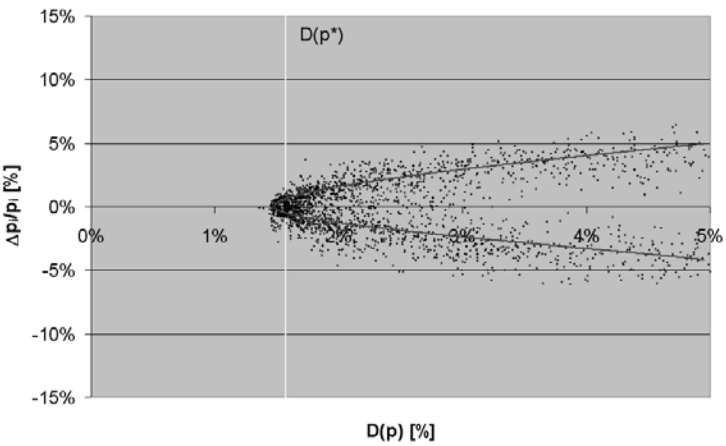

Figure IV-36 : Variation of D(p) vs. the variation of an influent parameter (Zoom)

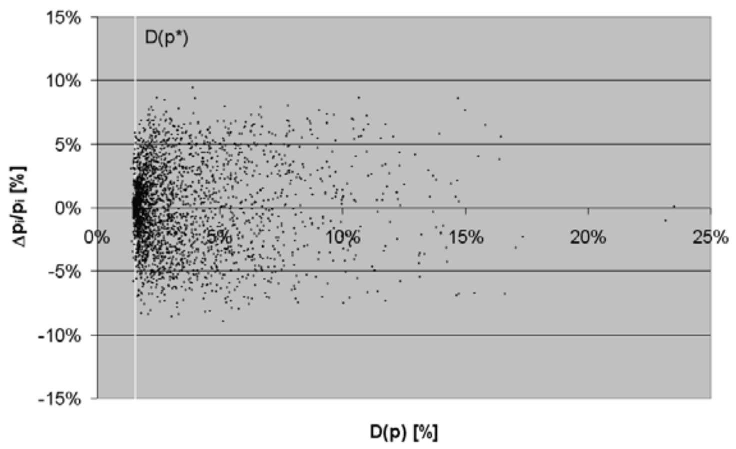

Figure IV-37 : Variation of D(p) vs. the variation of a non-influent parameter

Figure IV-35 and Figure IV-36 present the classical representation of an influent parameter and Figure IV-37 the typical cloud observable for a less influent parameter. The parabolic form highlighted by the line on Figure IV-36 marks the behaviour of an influent parameter on the matching quality. When this parameter moves away from its optimal position, either due to an increase or a reduction, there is a direct influence on the matching quality, the value of D(p) increases. Obviously, the match quality depends on the combination formed by the other parameters. On the other hand, Figure IV-37 displays the classical behaviour of a non influent or less influent parameter. It consists of a cloud with no clear trend. Most of the points are located close to the initial state (no variation, $\Delta p_i/p_i = 0$) and in the close vicinity of D(p*). That means that the current value is close to an optimised value and if the parameter is not too much modified, the matching remains in a range of good quality. Nevertheless, the lack of trend in the cloud of point indicates a poor influence of this parameter or its smaller influence compared to another parameter (like the preceding one).

For the analysis of the n parameters, only the most influent (often only one) governs the general quality of the matching. That means that only one or a few parameters presents a shape comparable to Figure IV-35 and Figure IV-36. Sometimes, when the optimisation is not completely done yet, the influent parameters display a general trend which is not a parabola centred on $\Delta p_i/p_i = 0$ but it can be a trend tending to the correct value of p_i. This trend could be linear or almost linear (Figure IV-38). Generally, when this case is observed, there is about half the total number of combinations that improve the matching quality. Figure IV-38 presents about 48% of the points enhancing D(p).

In conclusion, the parabola denotes an influent parameter close to its equilibrium position or optimised value. A straight line expresses a trend to be followed by an influent parameter and the cloud of points express a lack of relationships between the parameter variation and the matching fitting or the existence of a more influent parameter in the same sensitivity analysis.

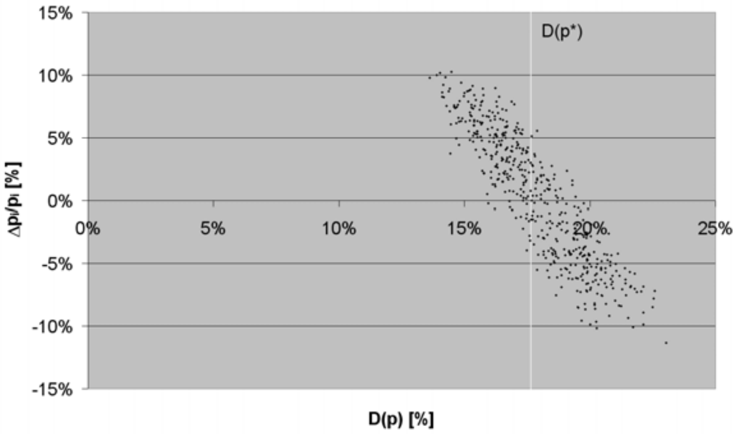

Figure IV-38: Variation of D(p) vs. the variation of a influent parameter

The variation of either the matching quality criterion or the variation of the sole parameters can be confronted with an another quantity linked to the main purpose of the analysis.

These quantities could be:

- The ultimate state of the soil reaction mobilized along and beneath the pile (Figure IV-39);
- The load corresponding to a given settlement (Figure IV-40);
- The settlement corresponding to a given applied load;
- The secant stiffness of the simulated load settlement curve for a given load or displacement;
- Other quantity depending of the parameters studied.

Figure IV-39 and Figure IV-40 present two possibilities of these combinations: the variation of the ultimate soil reaction expressed as a function of the matching quality factor and the evolution of the load corresponding to a settlement of 15 mm as a function of the variation of a parameter of the model

The calculation of the load for a given settlement and inversely, the calculation of the settlement for a given load are two algorithms developed by the author and allowing to know a particular point of the static load-settlement curve without the construction of all the curve.

When the matching quality factor is close to its minimum and the set of parameters is in the area of its optimum, Figure IV-39 and Figure IV-40 look like a parabola.

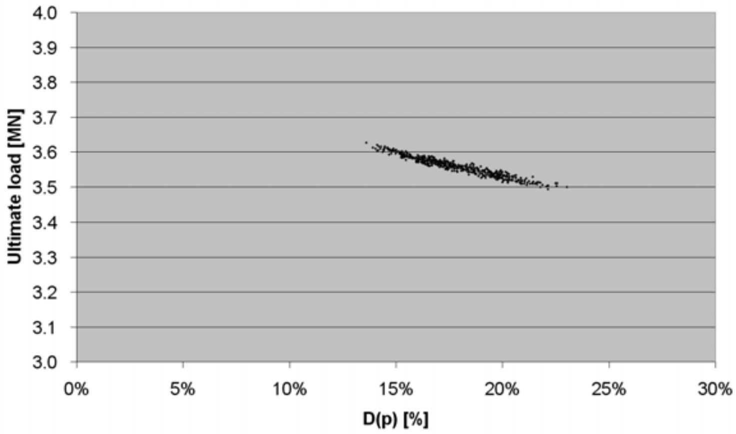

Figure IV-39 : Variation of the estimated ultimate pile capacity vs. the matching quality factor D(p)

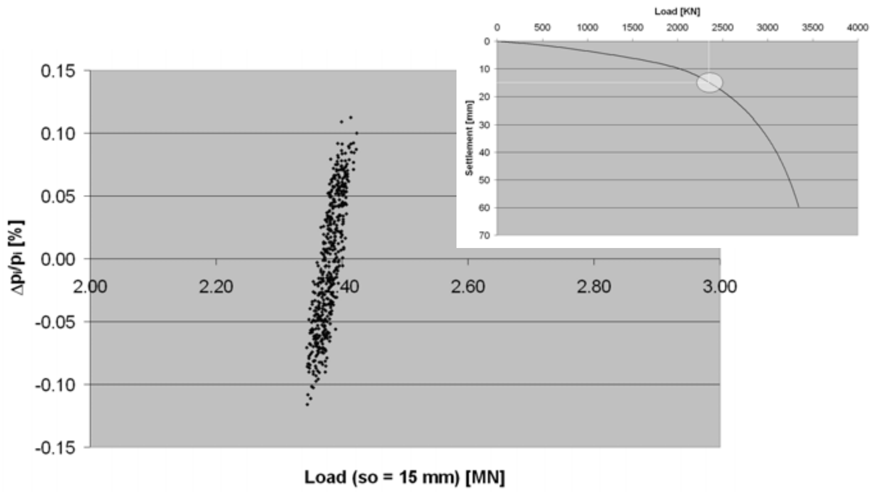

Figure IV-40: Variation of an influent parameter vs. the load corresponding to a head settlement of 15 mm.

4.2. Classification of the parameters due to their relative influence

Since all the parameters influence differently the pile/soil response, and since the most influential parameters lead the optimisation process, it is important to identify the weight of each parameter on the matching process in order to select them correctly and to find out the best solution for each of them. After a complete analysis of real cases from Sint-Katelijne-Waver and Limelette, it appears that the most influential parameters are characterized by a parabolic cloud of generated points similarly to Figure IV-36 and that the others parameters do not show a particular trend like on Figure IV-37. Figure IV-41 to Figure IV-44 present the results of clayey and sandy sites for both influent and non-influent parameters.

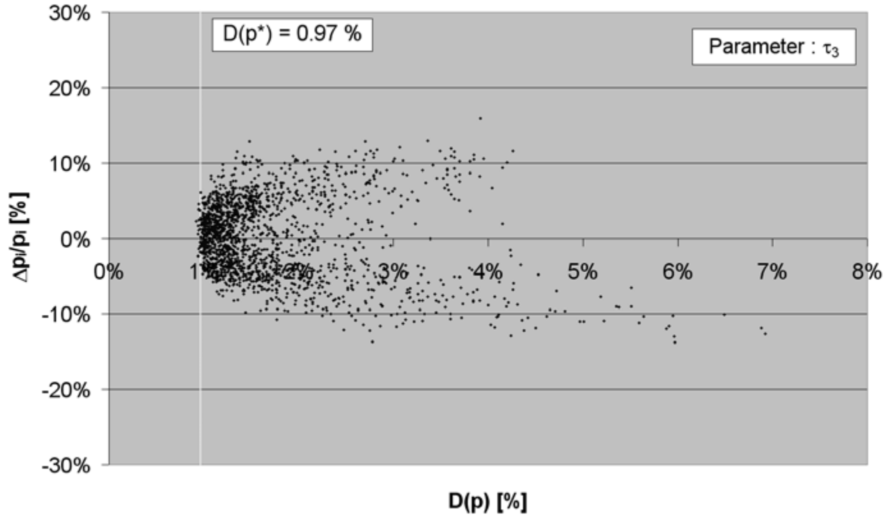

<u>Figure IV-41</u>: Variation of the parameter τ_3 (ultimate strength of the 3rd layer) vs. the matching quality factor D(p) – clayey site

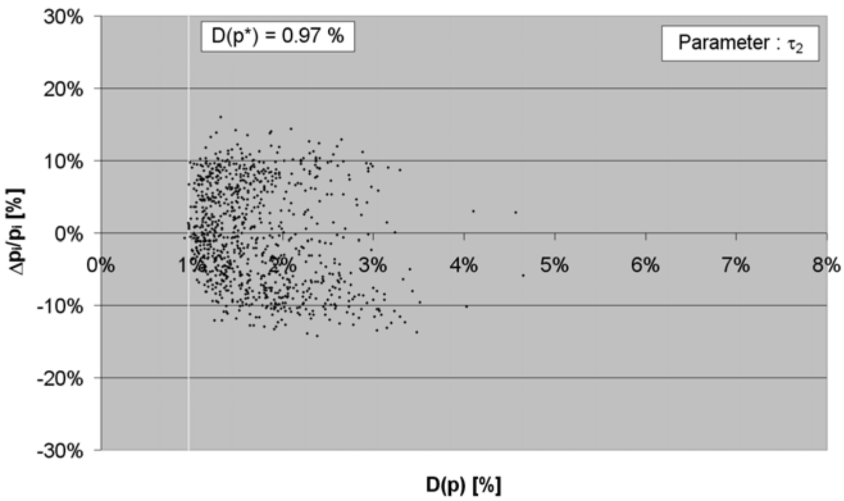

<u>Figure V-42</u>: Variation of the parameter τ_2 (ultimate strength of the 2nd layer) vs. the matching quality factor D(p) – clayey site

The consequence of this influence is a good optimisation of the concerned parameters (the most influential) and a poor optimisation of the others parameters. The less influential parameters remain almost unchanged after processing.

Nevertheless, it is possible to improve their optimisation by retrieving the most influential parameters and by launching a new optimisation process on the remaining parameters. A new balance between parameters is performed and a classification can be done based on this hierarchy of influent parameters. A major consequence is that the less influent parameters, like the damping factors J_i at the base and along pile shaft, can be optimised.

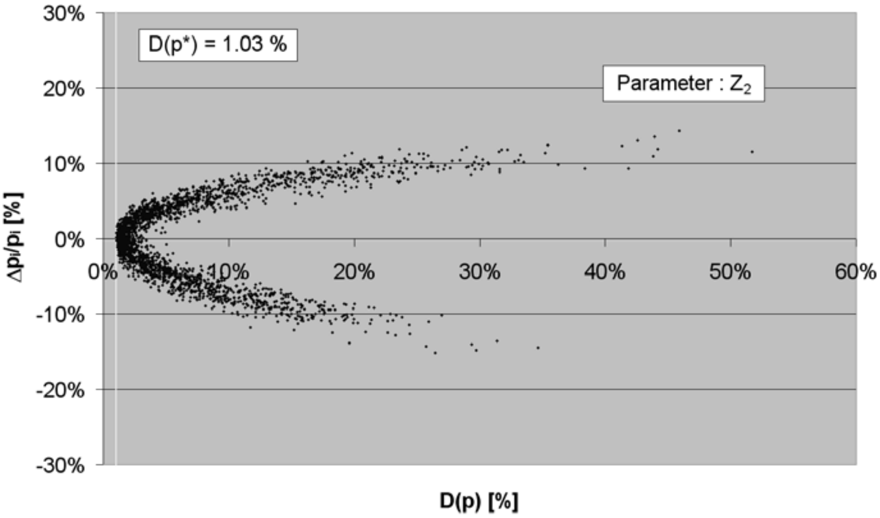

<u>Figure IV-43</u>: Variation of the parameter Z_2 (depth of the 2nd layer) vs. the matching quality factor D(p) – sandy site

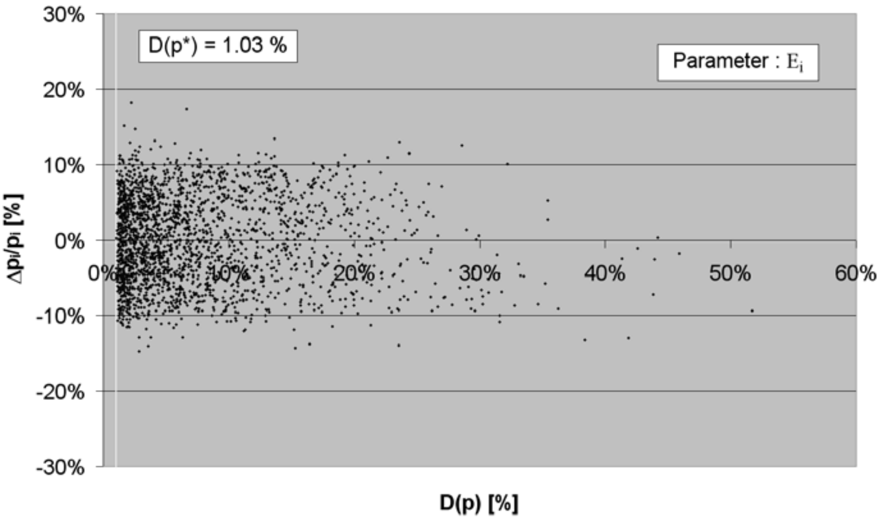

<u>Figure IV-44</u>: Variation of the parameter E_i (elastic modulus at the pile base) vs. the matching quality factor D(p) – sandy site

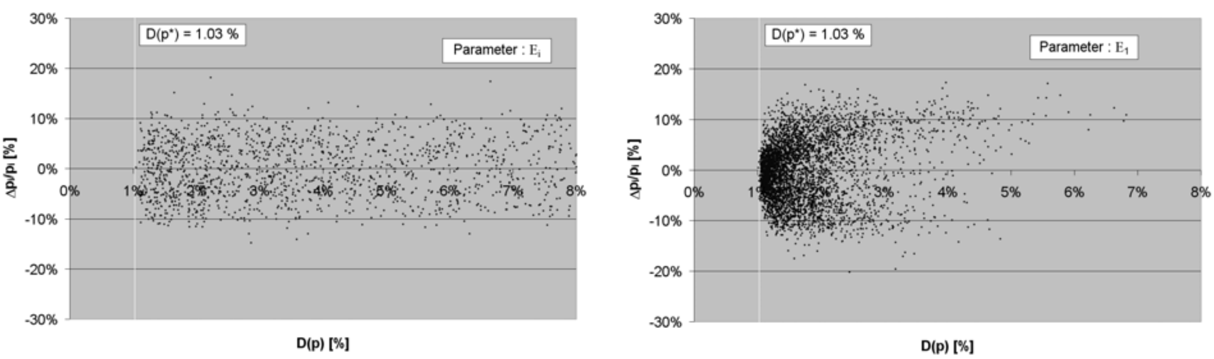

<u>Figure IV-45</u>: Comparison of the variability of E_i with and without a more influential parameter – sandy site

Figure IV-45 highlights the hierarchy existing between the parameters through their relative influence on the pile/soil response. Both figures show the analysis of the same parameter with and without a most influent parameter. the left figure presents a cloud without trend, the right figure highlights the influence and allow to refine its optimisation.

Despite the large influence of some of the parameters (principally the parameters linked to the static soil resistance like the thickness of the shaft layers or the ultimate strength of the shaft layers), it is possible to perform an optimisation on all the pile/soil model parameters, even the less influential like the rheological ones.

Figure IV-46 and Figure IV-47 present similar figures where the same parameter is shown with and without the influence of a more influential parameter. This allows the discernment of an optimised value.

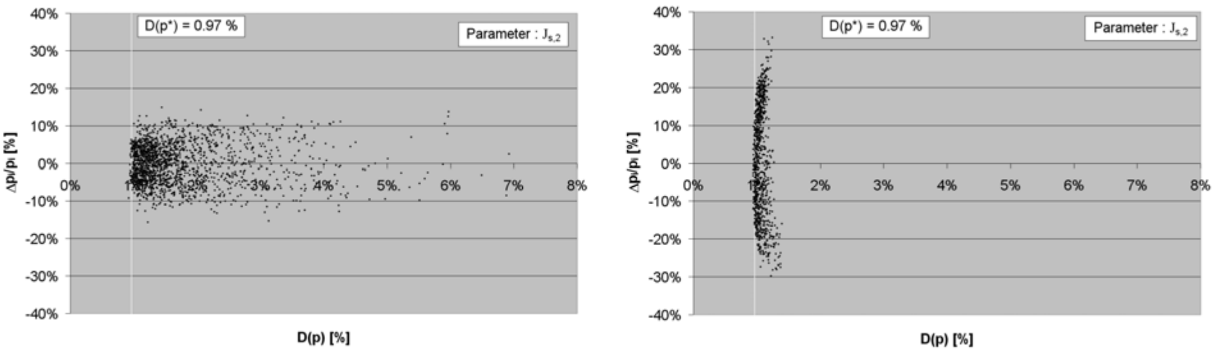

Figure IV-46: Comparison of the variability of $J_{s,2}$ (shaft damping factor of the 2nd layer) with and without a more influential parameter – clayey site

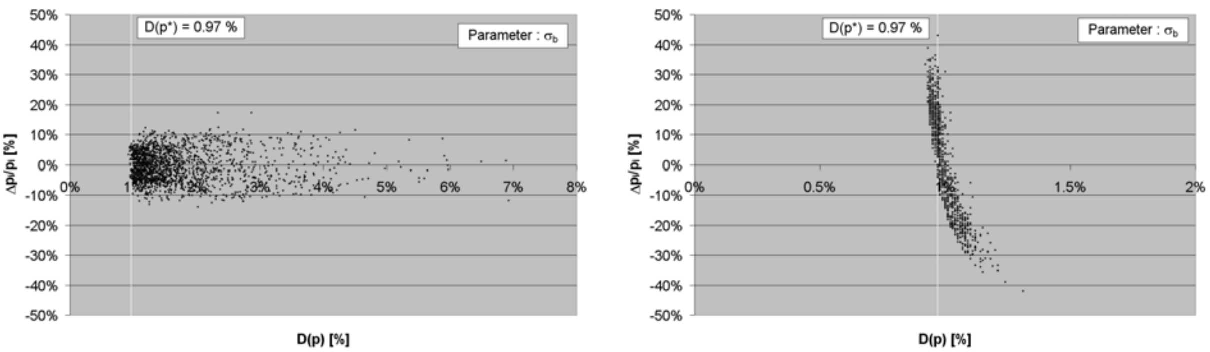

Figure IV-47: Comparison of the variability of σ_b (ultimate vertical stress at the pile base) with and without a more influential parameter – clayey site

5. Results of the back-analysis on real measurements

In order to illustrate the back-analysis process, the dynamic tests performed on the two sites are analysed. A complete set of DLT blows has been analysed for each type of soil and the results are displayed in the two next sections. One for the Sint-Katelijne-Waver (Boom clay) and one for Limelette (Bruxellian sand).

5.1. Analysis of the dynamic tests from Sint-Katelijne-Waver

The tests analysed are those already studied in chapter 3. It concerns the long prefabricated pile A7 described in detail in section 3 of chapter 3. The pile is 13 m long and its embedded part is 10.9 m long. The base is located at 11.63 m of depth.

The modelled pile is decomposed in 10 elements, the pile modulus of elasticity is fixed to 38000 MPa (c = 3940 m/s) and the surrounding soil is described by the input set of parameters (Figure IV-9 to Figure IV-11). The exponents N of the velocity dependent power laws are fixed to 0.2 for the shaft and 1 for the base according to the results obtained in literature. These values are not optimised and remain fixed during all the process. The ratio of shear modulus G_2/G_i describing the unloading is fixed to 1 and authorized to be optimised. The input set of parameters is the same for each analysis. Each blow is considered as an independent study.

The pile A7 was tested twice with about one year of delay between the testing campaigns. The first has been carried out in 1999 and the second in 2000. As it was described in section 3.3 of the chapter 3, only the first blows of the second campaign are valid because of an extreme eccentricity. But the blows of both campaigns are similar with no pronounced difference. Since the first blows of the 2000's campaign were very weak (0.2 m to 0.6 m of drop height) the three first blows analysed come from this campaign, they are called A7b-00i. After, tests of the 1999's campaign with higher drop heights are analysed (called A7-00i). Table IV-3 informs of the chosen blows, of the drop heights and of the maximum and permanent settlements reached during each blow according to the analysis of the acceleration measurements at the pile top (more details in section 3.3 of chapter 3). There are 6 blows from 0.2 m to 1.6 m.

	Drop Height [m]	Max Settlement [m]	Perm Settlement [m]
A7b-001	0.2 m	0.0021 m	0.0001 m
A7b-002	0.4 m	0.0039 m	0.0002 m
A7b-003	0.6 m	0.0052 m	0.0003 m
A7-002	0.8 m	0.0062 m	0.0012 m
A7-003	1.2 m	0.0086 m	0.0027 m
A7-006	1.6 m	0.0109 m	0.0039 m

Table IV-3: Summary of the analysed blows and of the reached settlements.

The back analysis is processed by the automatic algorithm proposed in this research. The matching procedure is performed by optimisation of all the parameters in the same time: since it is possible to refine the optimisation procedure to a certain number of parameters, Table IV-4 lists about the concerned parameters: 16 parameters.

Shaft (x 3 layers) :	$\tau_{ult,i}$	z_i	G_i	Js_i	G_2/G_1
Base 1 layer :	$\sigma_{ult,i}$	E_i	Jb_i		

Table IV-4: List of optimised parameters

The optimisation procedure start with a radius Δ of 90%, there are 10 reductions authorized and the last radius analysed is 5%. The number of iterations/radius without improvement of the matching quality factor D(p) is fixed to 100. The matching is processed on a duration of 15L/c which is sufficient for the tests in clay because of the dampening of the soil.

Table IV-5 presents the results of the matching procedure. D(p) is listed in %. This value is the sum of the weighted and averaged distance between the measured and calculated curves of force and velocity (Equ. IV- 2 and Equ. IV- 3). It can be seen that the quality decreases with the drop height.

	Matching factor D(p) [%]	Max inferred base settlement [m]	Difference max settlements pile top & base [m]
A7-001b	0.61 %	0.0007 m	0.0014 m
A7-002b	0.79 %	0.002 m	0.0019 m
A7-003b	0.98 %	0.0033 m	0.0019 m
A7-002	0.64 %	0.0045 m	0.0017 m
A7-003	1.06 %	0.0069 m	0.0017 m
A7-006	1.66 %	0.0092 m	0.0017 m

Table IV-5 : Results of the matching procedure (matching quality factor D(p)) and maximum base settlement obtained for each test.

Figure IV-48 to Figure IV-53 display the result of the matching procedure in terms of force-settlement curves. The measured one (Force measured – Set calculated) is compared to both calculated: "Force measured – Set calculated" or "Force calculated – Set measured". The quality is remarkable and the matching is successful for all blows. Nevertheless, it can be pointed out that the calculated settlement curves (based on the force signal as input) fit much better with the reference curve than the calculated force curves (based on the settlement as input). This trend increases with the height of drop and corresponds to the wave return after reflection at the pile base. The final maximum and final settlement are conserved. The energy (integration of the curve) is also well fitted. The matching is performed until stabilisation of the pile.

Figure IV-54 exhibits three couples of velocity curves: each couple includes the measured and the calculated curves of the blow #b001, b003 and 006. The agreement is perfect for the tests with small drop height (#b001, b003), and the agreement is less perfect with the more energetic blow, the second peak of velocity is particularly difficult to be modelled where this peak is almost missing in the two others curves. Since this second peak is a consequence of the wave propagation and especially the reflection of the wave at the pile base and free top, it must be correlated.

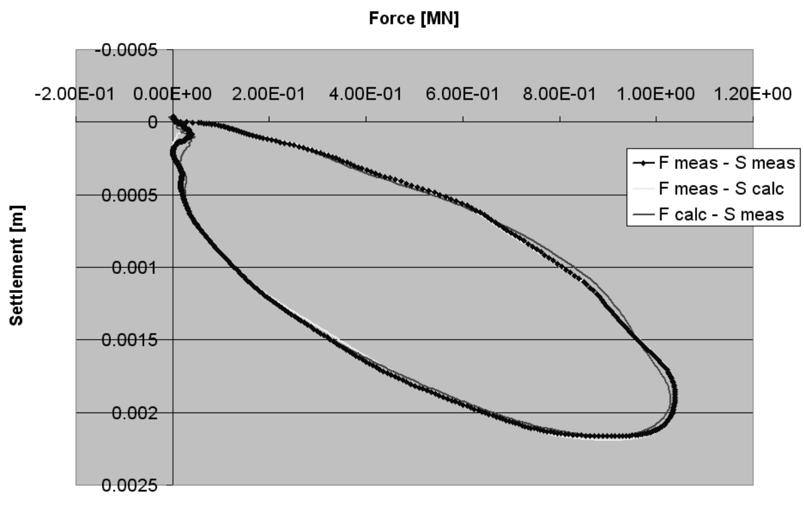

Figure IV-48 : Force-settlement curves (measured, and optimised (2 curves)) – blow A7b-001/ 0.2 m.

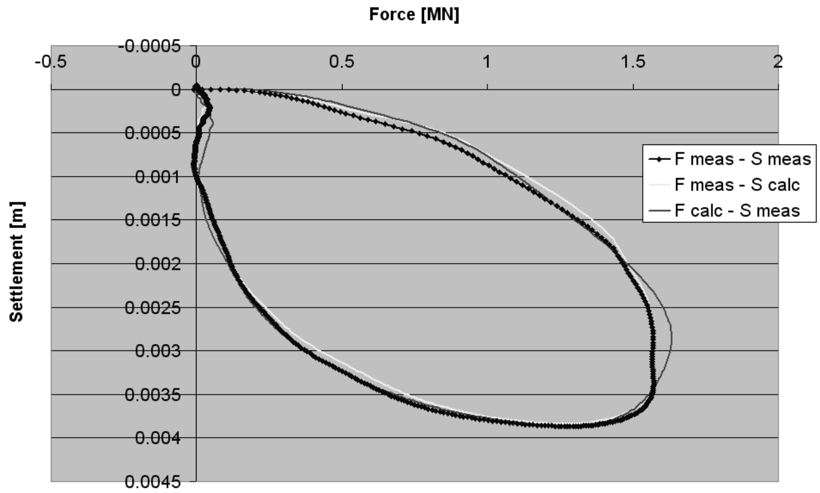

<u>Figure IV-49</u> : Force-settlement curves (measured, and optimised (2 curves)) – blow A7b-002/ 0.4 m.

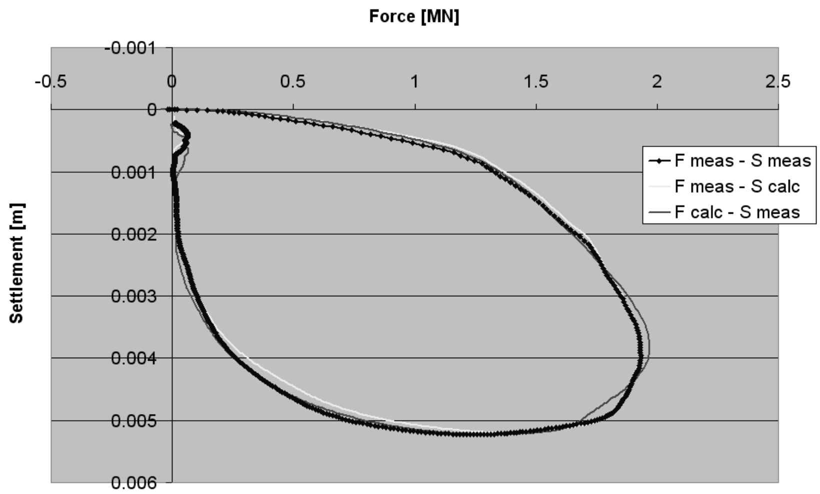

<u>Figure IV-50</u> : Force-settlement curves (measured, and optimised (2 curves)) – blow A7b-003/ 0.6 m.

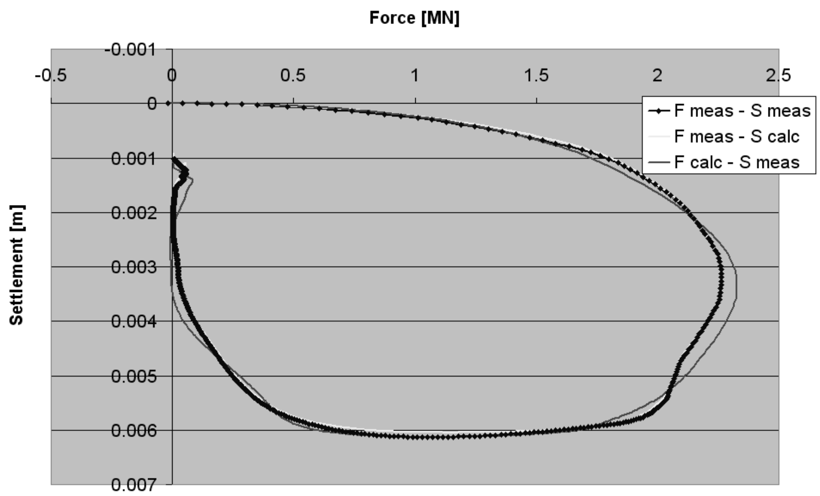

<u>Figure IV-51</u> : Force-settlement curves (measured, and optimised (2 curves)) – blow A7-002/ 0.8 m.

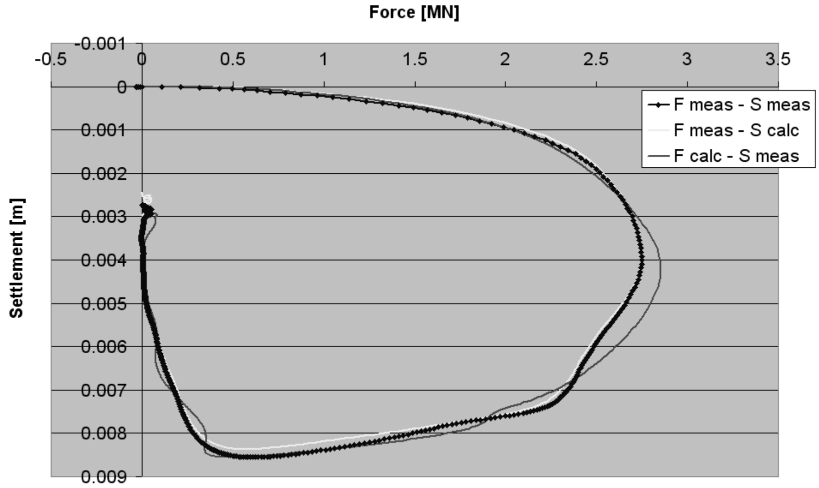

Figure IV-52 :Force-settlement curves (measured, and optimised (2 curves)) – blow A7-003/ 1.2 m.

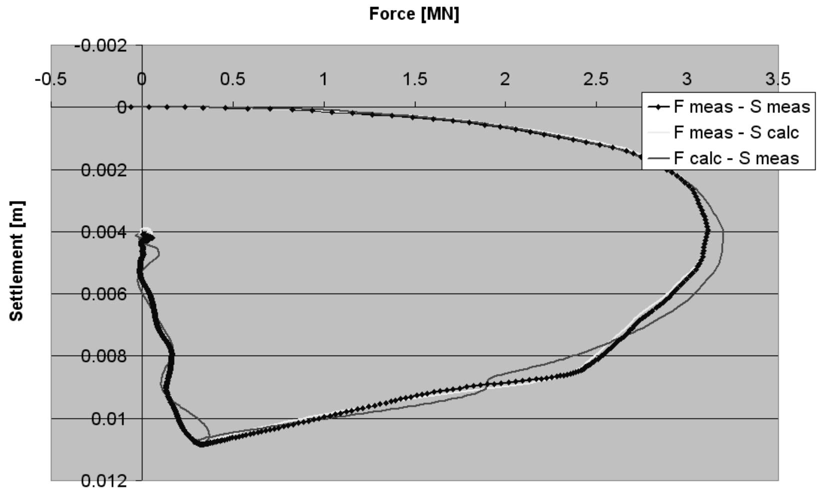

Figure IV-53 : Force-settlement curves (measured, and optimised (2 curves)) – blow A7-006/ 1.6 m.

The code allows to check the fundamental stress-displacement relationship mobilized for all pile elements by selecting one of them to observe the plot or by storing it. The behaviour of the last element close to the pile base was investigated and the maximum settlement of this last element is listed in Table IV-5 for each analysis. The maximum settlement increases with the drop height. Hence, the transfer of load to the base is also increasing. The total shortening of the pile is the difference between both maximum settlements and is listed in Table IV-5. It is seen that this shortening is constant for the three tests of the first campaign (002-003 & 006) and also constant for the two higher drops of the 2nd test campaign. this difference, even small, can correspond to a change in the pile/soil interaction system (distribution of load, or modification of the ultimate soil resistance, or stiffness). But the constancy of the shortening for all blows is also the mark of the constancy of the mobilization of the soil reaction along the pile shaft. It can be assumed that if the mobilized shaft reaction is constant, that means it could correspond to the ultimate one. More details are available with the integration of the reaction mobilized along the pile (Figure IV-69).

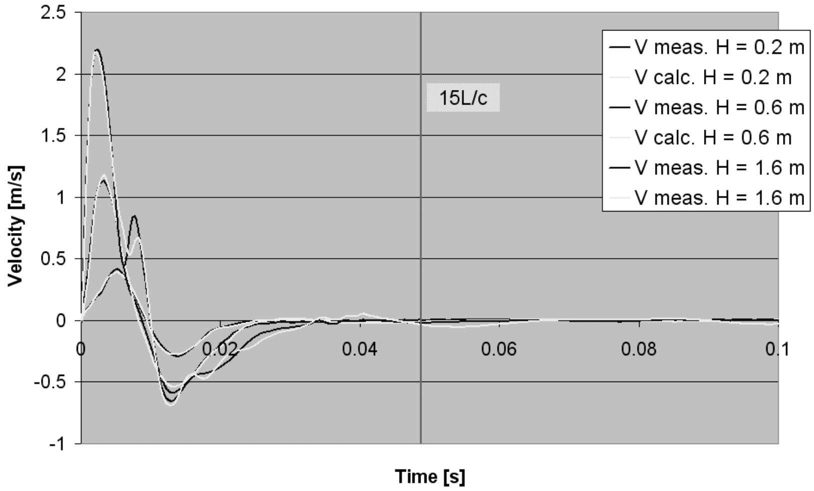

Figure IV-54 : Velocity curves (measured, and optimised) – blows A7b-001/ b-003 & 006

Before describing the distribution of the soil reaction along the pile shaft, most resistant part of the pile capacity for a pile in clay, Figure IV-55 presents a summary of the result of the base parameters optimisation. The histograms display 4 types of data, the height of drop being reminded for each blow:

- The maximum static stress reached at the base during the test σ_{max};
- The base damping factor J_b;
- The initial elastic modulus E_i;
- The ultimate vertical stress under the base, labelled in text box in the middle of the bars σ_{ult};

Trends, expected or not, can be highlighted.

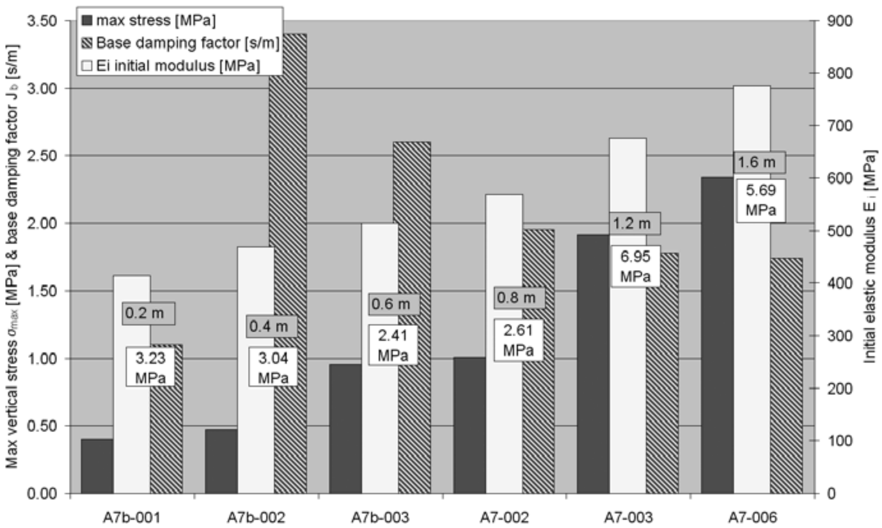

Figure IV-55 : Description of the base parameters after optimisation

The maximum stress σ_{max} reached increases with the drop height, as expected and denotes an increasing base mobilization but the corresponding ultimate value σ_{ult} increases as well what is not wished. The base damping factor has no influence in the first test because the base is almost not mobilized by the load transmitted through the pile. The load is almost completely transmitted to the shaft (displacement of max 0.7 mm for the base for the blow A7b-001). But from the drop height of approximately 0.8 m, the sensitivity analysis of the base damping factor shows a pronounced trend of about 1.8..1.75 s/m which is stable and significant compared to the smallest drop height. It is remarkable tot see that the base damping factor decreases with the increasing drop height from a very high value (J_b = 3.4 s/m) to a stable one for large drop height. On the other hand, the initial elastic modulus has an upwards trend with the height of drop which can be linked to the stiffening of the soil.

The soil reaction along the pile shaft is summarized with all the data available:

- The profile of the local shear strength f_s measured with the CPT;
- The step profile introduced as input (in dashed lines) τ_{ult};
- The step profile of the ultimate shear strengths obtained after optimization τ_{ult};
- The step profile of the maximum reached shear stresses along the pile shaft τ_{max};
- The values of the initial shear modulus G_i for each soil layer;
- The value of the shaft damping factor J_s corresponding to each soil layers.

There is one figure per test (Figure IV-56 to Figure IV-63). In order to perform a global analysis, each figure is analysed individually and afterwards, the main remarks are summarized.

A7b-001: 0.2 m

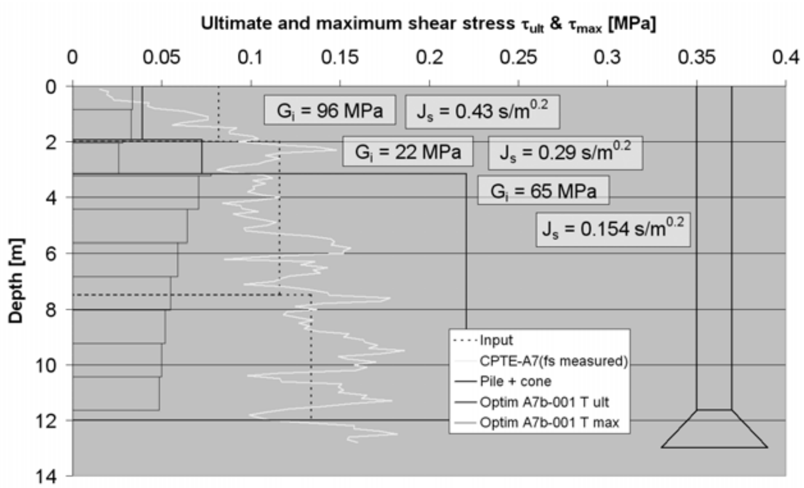

Figure IV-56: Summary of the parameters of the soil reaction along pile shaft for the blow A7b-001

Remarks:

- The ultimate profile optimised is rather different compared to the reference one but it is expected due to the small height of drop, the small settlement generated (0.2 m – 21 mm at the pile head – 0.7 mm at the pile toe) and the consecutive soil mobilization;

- The values of the shear modulus G_i are abnormal, especially for the 2nd and the 3rd layers. 22 and 65 MPa are not high enough;

- The profile of the maximum reached shear stress is increasing with the layers but decreasing with depth in the same layer. This is due to the shortening of the pile element and the reduction of the their respective motion; However, the small value of the second maximum reached stress is inferior to the first one; this is not correct and due to the low value of the shear modulus $G_{i,2}$;

- The levels of reached stresses are low compared to their corresponding ultimate values. This is a direct consequence of the small shear modulus and the reduction of the pile elements motion with depth;

- The values of J_s for the three layers can be characterised by a sensitivity analysis (Figure IV-57). Only the first damping factor has a significant influence on the matching quality (not necessarily an improvement, but a trend like those observed on Figure IV-35 and Figure IV-36). The two next ones do not mobilize their ultimate rheologic resistances, mainly because the level of velocity of each pile element is not sufficient to generate a radiation term of importance able to exceed the ultimate rheologic resistance. Since the maximum static reached stress of the first layer is close to its ultimate one, the failure occurs. The value of $J_{S,1}$ minimizing the matching quality factor is equal to 0.43 s/m$^{0.2}$ +/- 15%.

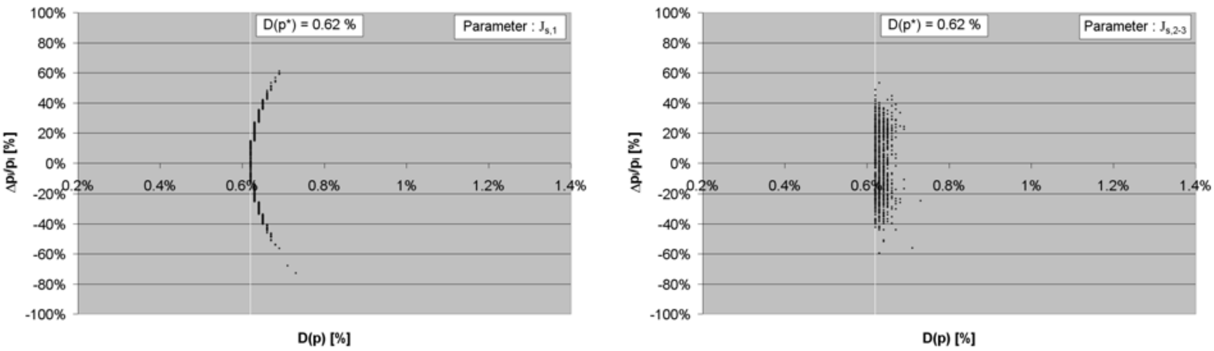

Figure IV-57 : Sensitivity analysis of the shaft damping factors $J_{s,I}$

<u>A7b-002 : 0.4m</u>

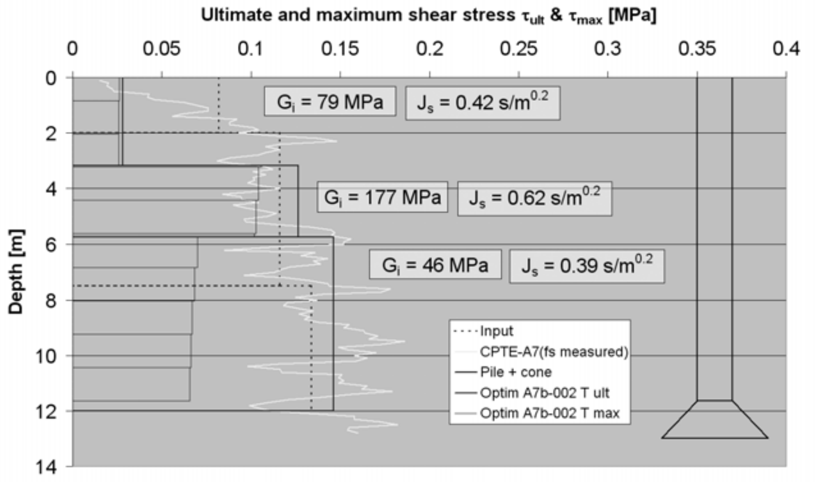

<u>Figure IV-58</u> : Summary of the parameters of the soil reaction along pile shaft for the blow A7b-002

Remarks:

- The optimised ultimate shear stress profile is close to the CPT and the reference ones;

- On the other hand, the maximum reached values profile displays a decreasing trend with depth; this is not expected;

- The first layer of soil is fully mobilized in static, and also in dynamic. The shaft damping factors of the two first soil layers are both considered as influent on the matching quality criterion (<u>Figure IV-59</u>); $J_{S,1}$ and $J_{S,2}$ are fixed to 0.42 s/m$^{0.2}$ and 0.62 s/m$^{0.2}$ respectively. These values, and especially $J_{S,2}$ must be kept in mind for the future characterisation of the dynamic properties of the Boom clay.

- The profile of initial shear modulus G_i is still odd. The second layer is 4 times stiffer than the layer underneath. The stiffness evolution with depth is rather unusual and does not correspond to the reality.

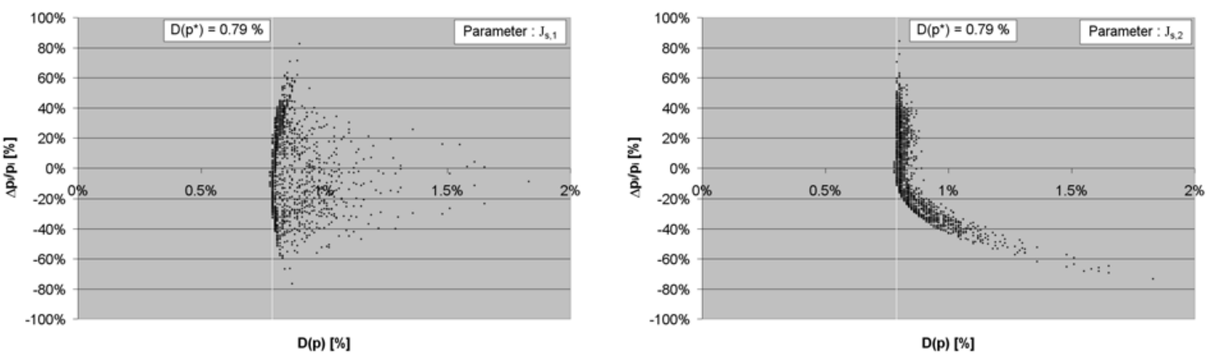

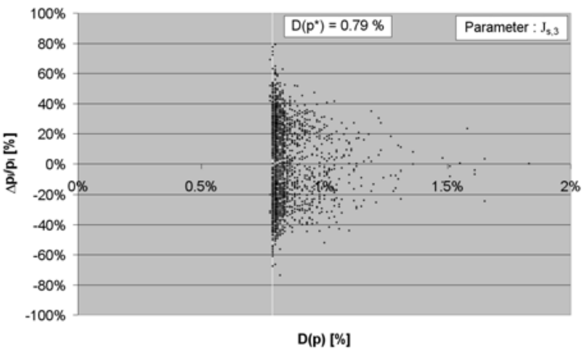

Figure IV-59 : Sensitivity analysis of the shaft damping factors Js,i

A7b-003: 0.6 m

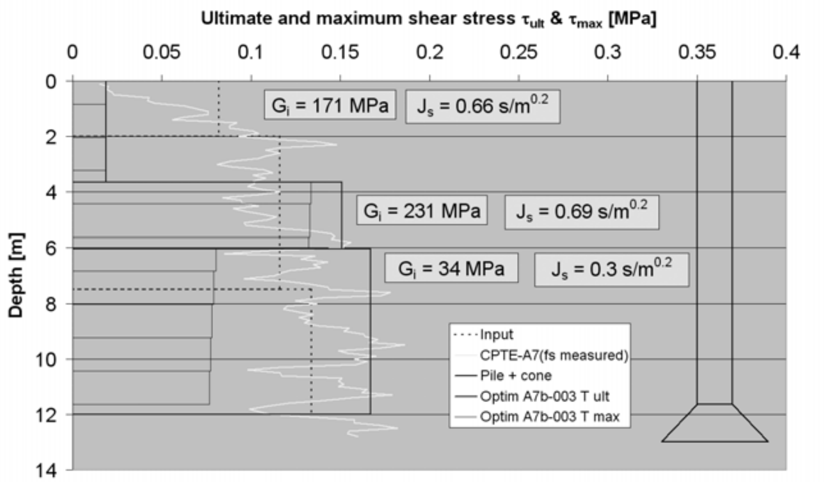

Figure IV-60 : Summary of the parameters of the soil reaction along pile shaft for the blow A7b-003

This analysis exhibits the same remarks than the previous ones:

- A good ultimate stress profile. But the first layer becomes more and more degraded;
- An illogical profile of stiffness with the lower value close to the pile base;
- A profile of maximum reached shear stresses also inverted;
- Values of shaft damping factors significant for the two first layers and insensitive for the third one (result obtained by means of a sensitive analysis similarly to Figure IV-59).

A7-002: 0.8 m

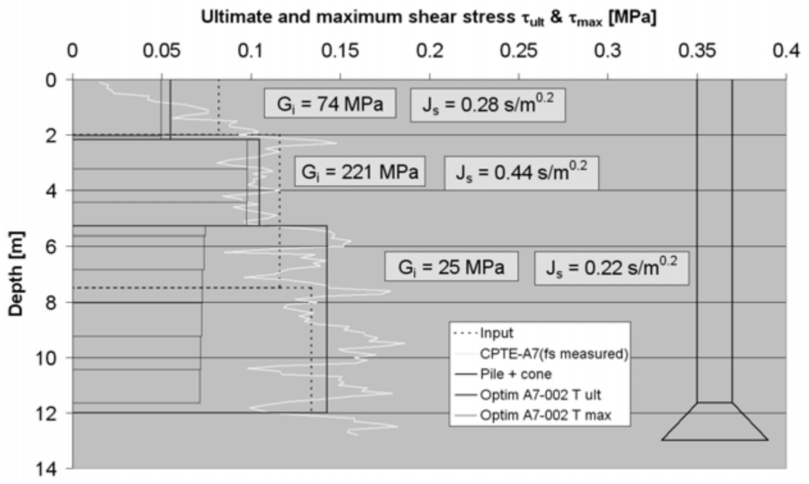

Figure IV-61 : Summary of the parameters of the soil reaction along pile shaft for the blow A7-002

The main results are similar to the previous ones. The 3rd layer starts to slightly influence the matching quality. This is due to the increasing velocity at the pile top and along the pile shaft. This increases the relative influence of the radiation damping in the rheologic stress evaluation. On the other hand, the 1st layer has less influence because of its small thickness compared to the pile length and the relative influence of the others layers.

A7-003 : 1.2 m and A7-006: 1.6 m

Still the same remarks with a smaller value of the shear modulus of the 3rd layer (14 and 15 MPa respectively).

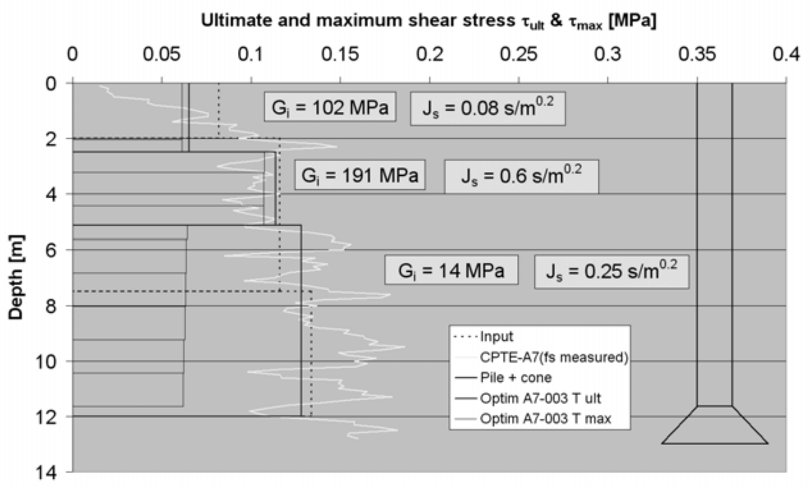

Figure IV-62 : Summary of the parameters of the soil reaction along pile shaft for the blow A7-003

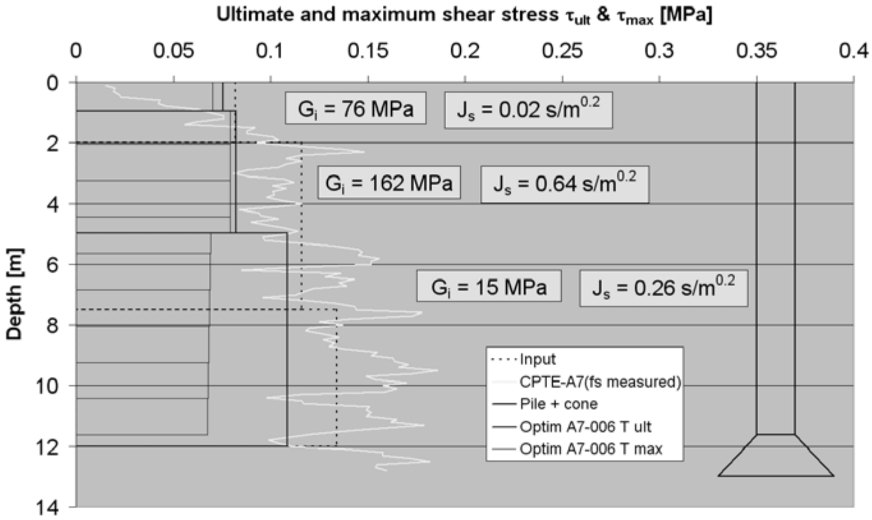

Figure IV-63 : Summary of the parameters of the soil reaction along pile shaft for the blow A7-006

Summary:

- The ultimate profile is remarkably close to the theoretical situation in the field but both maximum reached shear stress and shear modulus profiles are illogical and irrealist.

- The shaft damping factors are also remarkably stable through all the analysis performed. If only the second layer can be considered as reliable due to the expected values of shear resistance and shear modulus, the value of 0.6 s/m$^{0.2}$ can be representative of the site (including the pile, the soil type and the level of energy). Moreover, these values were refined after the first phase of optimisation by mean of a sensitivity analysis allowing a precise optimisation of a few number of parameters (Figure IV-57 and Figure IV-59). Nevertheless, the unusual profiles, the low values of G_i prevent to be categorical.

The ratio of shear modulus G_2/G_i [2] are listed for all the tests:

	G_2/G_i
A7-001b	0.64
A7-002b	0.29
A7-003b	0.25
A7-002	0.25
A7-003	0.28
A7-006	0.3

Table IV-6 : List of unloading shaft ratio G_2/G_i

These values are extremely small and do not support a physical behaviour, because of energy considerations.

The combination of the initial shear modulus, the ultimate shear stress, the ratio of shear modulus G_2/G_i and two hypotheses of the pile/soil model allow to bring some insight into the situation. These

[2] The quotient of the unloading initial shear modulus to the loading one. If the quotient is >1, the unloading is stiffer than the loading; the expected situation is a ratio > 1.

two hypothesis express that the ratio of shear modulus G_2/G_i is the same for all soil layers, and that the pile is moving into a fixed soil considered as motionless. Since the soil reaction is determined by its mobilization, the stress generated at the interface with the pile is determined by both relative displacement and velocity. Since the soil is motionless, the relative displacement becomes the pile displacement. There is no possibility of slippage, because the slippage is, by definition, the relative movement of a body with respect to another. So, the stress of a soil particle and the displacement of this soil particle are linked.

However, the pile motion is determined by the input condition (integration of the velocity of the pile head). There is also a force balance at the pile head between the external force (from the blow) and the internal forces (from the soil reaction). This balance acts at the pile top but also influences each node of the pile. Finally, since the pile is mechanically known (pile material elastic modulus, dimensions, stiffness,…), the pile top constraints are transmitted at each node (force and displacement) according to the local modifications (elastic shortenings,…). So the pile must globally respect a force equilibrium and a settlement balance corresponding to the input information. And, the soil must respect the same constraints.

The soil behaviour is characterized by its stress-displacement relationship. This relationship is function of 3 interconnected parameters[3]:

- The ultimate soil resistance;
- The initial shear or elastic modulus;
- The unloading ratio of shear or elastic moduli.

Since the pile displacement and then, the soil displacement is defined by the settlement balance at each node, since the reached stress is also defined by the force equilibrium, the only parameters variable in order to minimize the matching quality factor are the ratio of shear modulus, the initial shear modulus and the combination of the three parameters in order to keep constant the two conditions.

The pile element settlements during the blow A7-002 are plotted on Figure IV-64. All the elements follow the same trend led by the imposed signal at the pile head. The shortening of the pile and the progression of the wave into the pile are highlighted with the progression of the maximum settlement. The residual stresses generated along the pile shaft at the end of the blow are highlighted by the difference of permanent settlement of each pile's element. Those displacements are also the soil particle displacements at the interface. In order to ensure this displacement and the force equilibrium at each node during all the analysis duration, the variable parameters of the soil-displacement relationships are optimised[4]: the ultimate soil resistance and the initial stiffness for each soil layer, and the ratio of loading-unloading modulus. The result is given for two pile's elements on Figure IV-65 and Figure IV-66. The ratio G_2/G_1 is small and unphysical but imposed by the settlement and stress path conditions. If Figure IV-65 seems to be correct and representing an expected behaviour, on the

[3] In case of a hyperbolic or an elasto-plastic relationship.

[4] Plus the rheologic parameters

other hand, Figure IV-66 is completely illogic, especially during the unloading phase when the stress path goes over the loading stress path. That means that the unloading phase creates energy. This is physically impossible.

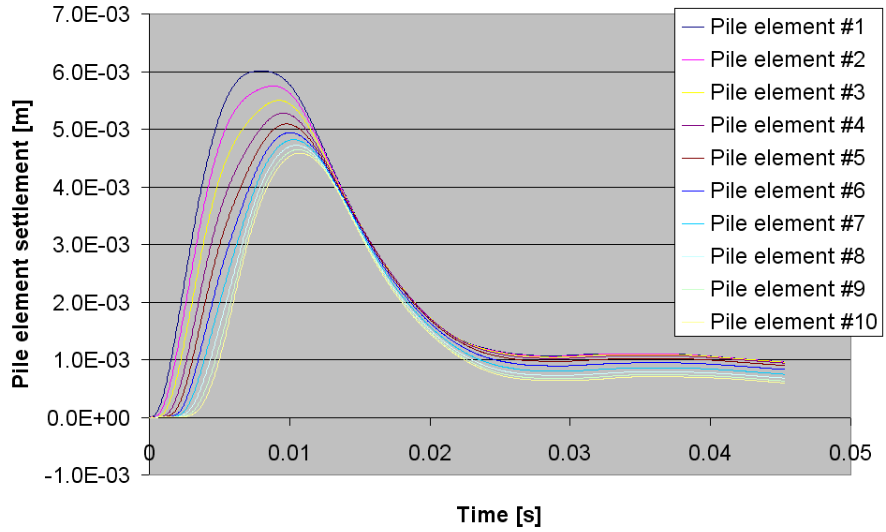

Figure IV-64 : pile's element settlement of A7-002

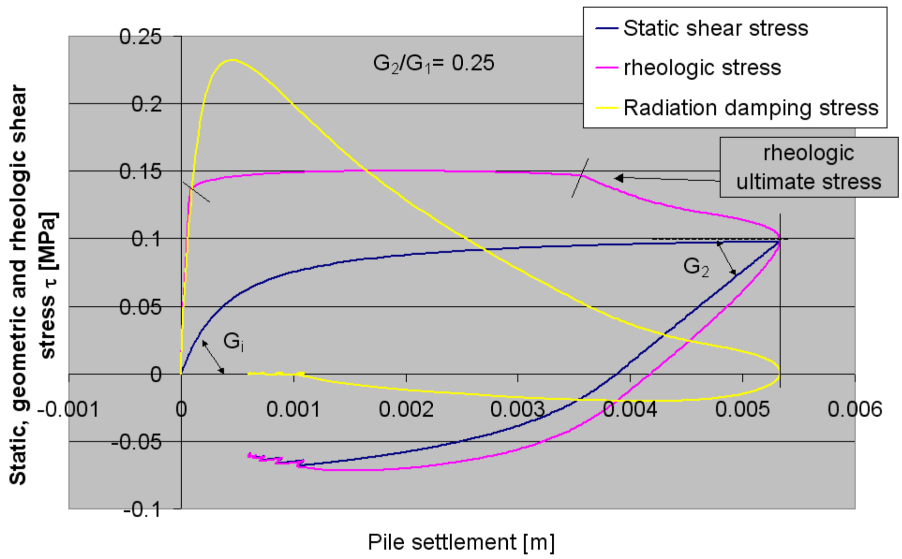

Figure IV-65: Detail of the soil reaction along the 4th element of the pile (blow A7-002)

The difference of behaviour is a result of the level of mobilization and the initial stiffness of the load-displacement curve.

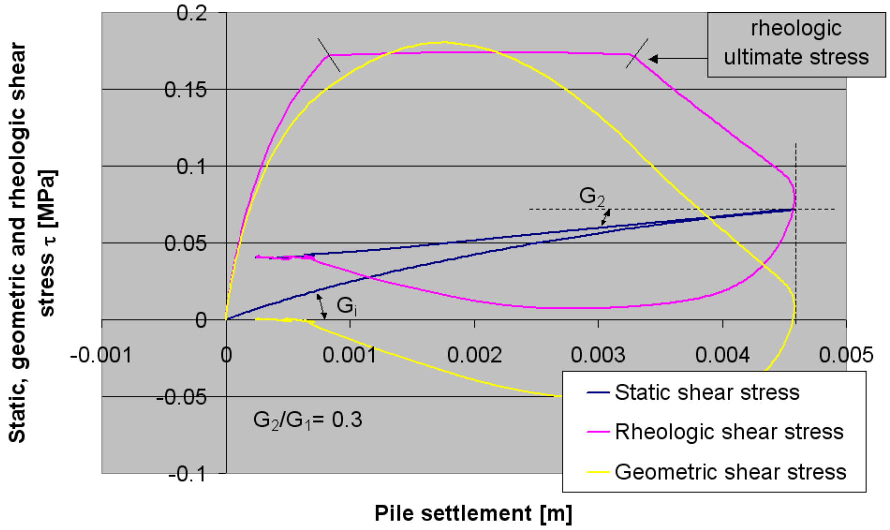

Figure IV-66: Detail of the soil reaction along the 13th element of the pile (blow A7-002)

If the initial shear modulus G_i are maintained fixed as given by the input, the optimisation gives a result where the ratio G_2/G_i is reduced to a very small value, the ultimate shear resistance of the last soil layer before the base is multiplied per more than 8 and the corresponding maximum stress of this layer reach unrealistic value compared to the real soil resistance (>> f_s (CPT)). Moreover, the matching quality can not be considered as successful (D(p) > 5%).

If the ratio of modulus G_2/G_i is fixed to 1 and maintained fixed during the optimisation, the last layer of soil describing the friction reaction includes almost all the pile length, the initial shear modulus is very low (less than 13 MPa) and the ultimate shear resistance is superior to the expected one (>0.3 MPa). However, the matching quality is correct and the pile's element settlement histories are very close to Figure IV-64.

The pile/soil model used does not allow to render the real behaviour of the pile/soil interaction. Whatever the initial conditions, it is impossible to have a final result respecting the ultimate resistance, the initial shear modulus profiles and an acceptable unloading modulus together in agreement with the reality. However, these conditions must be fulfilled in order to have the opportunity to optimise the rheologic parameters. Consequently, this problem must be solved by another way:

- To allow an independent unloading modulus for each pile soil element and to multiply the number of soil layers along the pile shaft;
- To work on a shorter duration including only the loading phase or the rebound stage of the settlement curve;
- To change the pile/soil model;

The first solution proposed was not followed because it does not answer to the underlying problem linked to the reliability of the modelling. If it is possible to match two curves by increasing the number of parameters, it is appropriate to improve the matching result by improving the model quality.

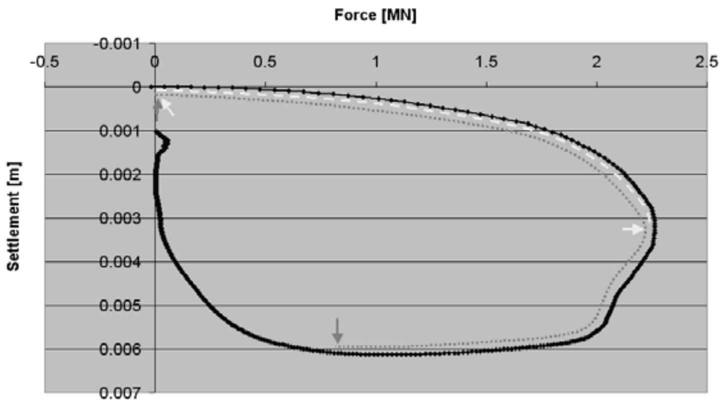

<u>Figure IV-67</u> : Optimization duration investigated

The second solution was widely investigated. The main idea was to focus the matching procedure on the reliable data. If the optimisation procedure is perturbed by the unloading stage, it can be possible to only analyse the loading stage, or the increasing part of the settlement (<u>Figure IV-67</u>). Unfortunately, the number of points before these two points is very low (less than 1L/c for the F_{max} analysis and less than 3.5 L/c for the S_{max} analysis) and does not enable a good optimisation process as possible.

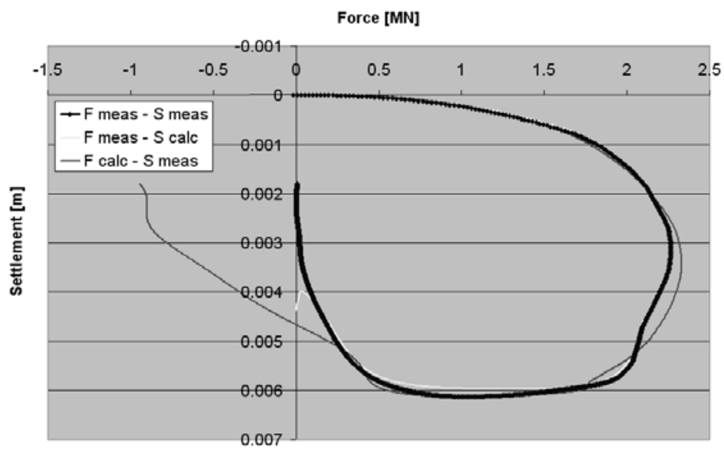

<u>Figure IV-68</u> : Influence of the optimisation duration on the matching quality

The following trend is noted: the longer the duration, the more pronounced the influence of G_2/G_1. If the duration is small enough, the unloading phase can be without importance. But if a short analysis allows one to optimise the parameters without modifying the initial modulus, the matching is relevant for this short duration and absolutely not for the rest of the signal (<u>Figure IV-68</u>).

Finally, the last solution proposed is the chosen one. Since the soil is considered motionless, the pile/soil interaction is lead by the pile motion without taking into account of the slippage into the formulations. This constraint links the loading and the unloading phases to the pile settlement. By authorizing the pile and the soil to move in an independent way, the interface motion between both media starts to have a certain magnitude when the pile slips into the soil. The pile/soil interaction must evolve to allow that. When the rheologic stress exceeds the ultimate rheologic resistance, the pile and the soil become uncoupled and both media behave independently (such an improvement is developed in the next chapter).

Other interesting results are available:

If the integration of the maximum stresses reached (static mobilization) during the blow along the pile and beneath the base is performed, <u>Figure IV-69</u> summarises all the analysed blows. The points inform about the evolution of the shaft friction with depth and the last point adds the base to the shaft soil reactions. The curves exhibit the evolution of the shaft friction mobilization with the height of drop. The blow A7b-001 (0.2m) shows a poor mobilization an a quasi nil base soil reaction. The A7b-002's

(0.4 m) shaft friction evolves and its base reaction increases a little. From the blow A7b-003 (0.6 m), the friction becomes almost identical for all the blows, only the base reaction presents an upwards trend.

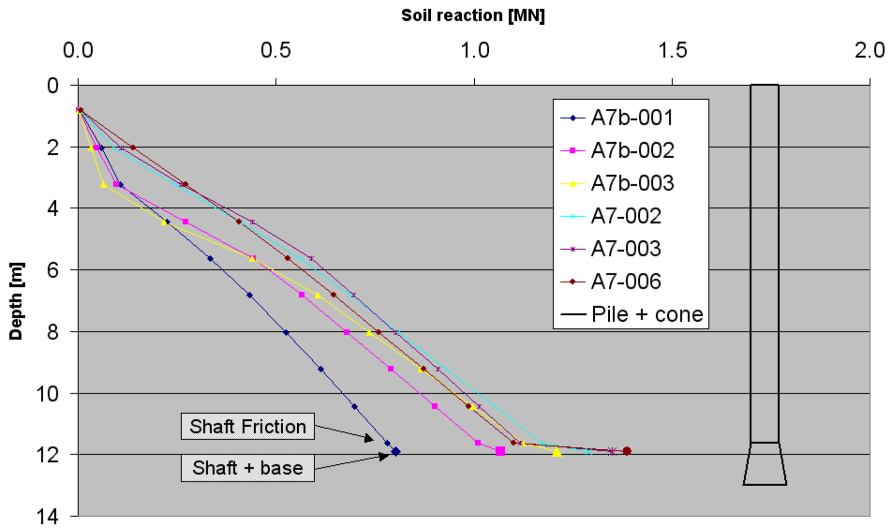

Figure IV-69 : Integration of the reached stresses along the pile and beneath the base for the analysis of Sint-Katelijne-Waver DLT tests

Despite the caution required due to the initial loading and unloading modulus problem (see above), the evolution of the blow analysis respects an expected trend: the progressive and quick mobilization of the shaft reaction, and the slower base reaction mobilization. This evolution isplotted vs. the maximum settlement measured of each blow (Table IV-3). Figure IV-70 exhibits this representation plus the separation of the total soil reaction in shaft and base terms and the corresponding static load-settlement curve measured during the Static Load Test performed on a identical pile in the close vicinity of the pile tested dynamically. The evolution of the integrated soil reaction is very close to the behaviour expected on clay: a very weak base resistance and a strong friction one quickly mobilized. The total soil reaction can be modelled by a hyperbolic curve which tends to an ultimate value of 1.7 MN. The comparison with the real curve prompts several observations:

- The initial stiffness is perfectly recovered;
- The large soil reactions are under-estimated compared to SLT result;
- The shaft friction curve present a recess after reaching a peak similarly to the observed behaviour during the static tests;
- The shaft friction seem to be fully mobilized after a settlement of about 6 mm, namely 1.5% of the pile diameter.

The same caution than previously must be kept in mind with this analysis due to the likely influence of the modelling of the initial modulus and the unloading phase on the integrated soil reaction. However, this representation has the advantage to condense all the analysis into a single figure (1 point/1 analysis).

Moreover, this kind of result is easy to plot and understand and is a usable result to easily compare the DLT conclusions to the SLT classic load settlement curve.

Besides the problem already approached, the under estimation could come from:

- The possible variation in the geotechnical profiles between the DLT and SLT locations;
- The base modelling with the cone of equivalent soil that underestimates the base soil reaction;
- The influence of the inertial and the load rate effects on the measured maximum settlements (overestimation of the measured settlement);
- The influence of the loading rate effect on the measured static load-settlement curve (overestimation of the measured load);
- Degradation of Boom clay under repeated impacts.

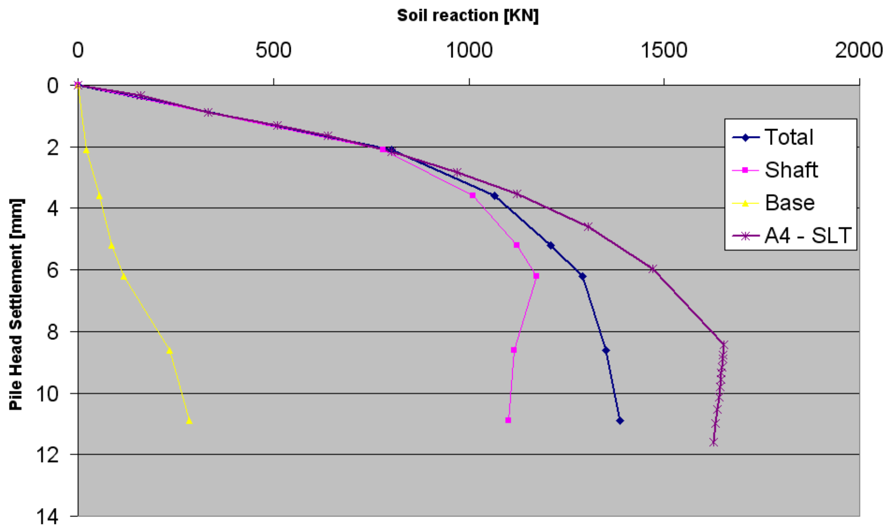

Figure IV-70 : Maximum mobilized load vs. maximum settlement for the sequence of blows A7 of SKW

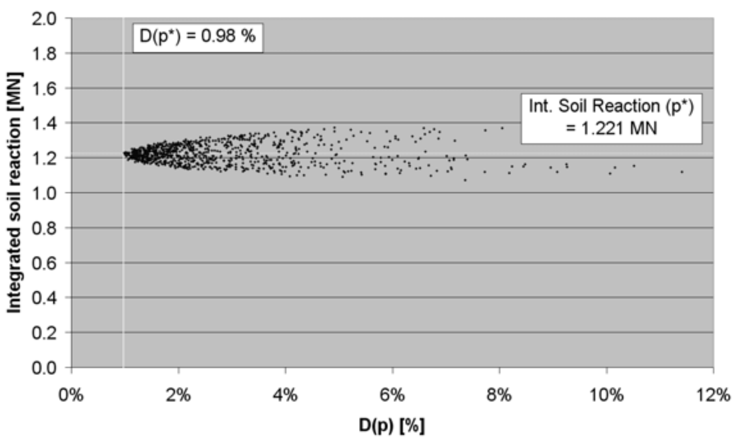

Figure IV-71 : Sensitivity of the integrated soil reaction of the blow A7b-003 around the optimal solution p*

A sensitivity analysis can be performed on the integrated soil reaction by varying all the parameters all around their optimal combination (p*) and to measure systematically the corresponding value of D(p) and the integrated soil reaction. Figure IV-71 exhibits this analysis for the blow A7b-003. The plot highlights the optimisation of the integrated soil reaction with the matching quality factor. That means that there is global balance between all the parameters to obtain a given matching linked to a certain soil reaction whatever the differentiation in shaft and base.

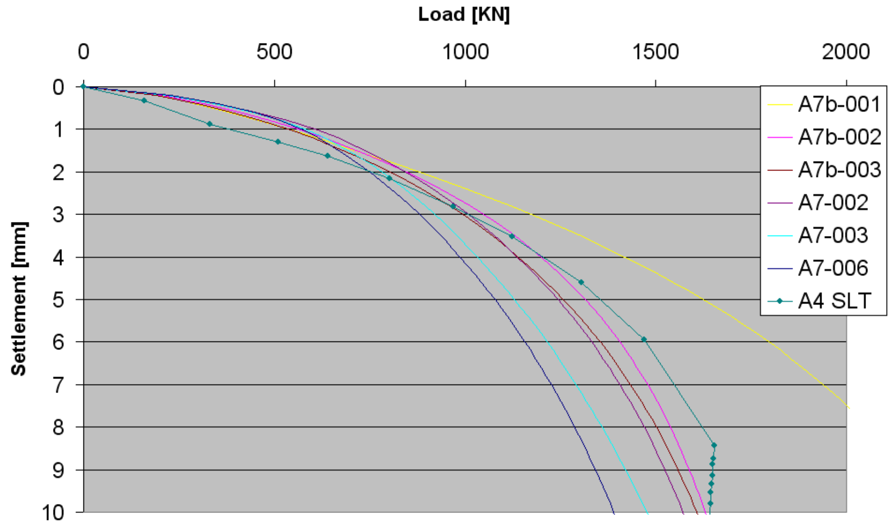

<u>Figure IV-72</u> : Simulation of the static load-settlement curves based on the individual analysis of the A7's blows

Finally, <u>Figure IV-72</u> summaries the simulations of the static load-settlement curves obtained from the individual analyses. The settlement axis is limited to 10 mm what is the maximum settlement reached during the dynamic tests analysed. The curve of the blow A7b-001 overestimates the static load settlement curve but the simulated curve must be compared until the mobilized settlement corresponding to the blow, namely 2.1 mm. At this settlement, the difference is not important. On the other hand, the curves of the higher drop heights are underestimated. It is probably a direct influence of the loading-unloading modulus. The others curves are very similar and present a good quality of simulation in the range of the concerned settlements. The initial stiffness of the curve is higher than the SLT due to the high values of initial shear modulus in the first layers, but this tangent stiffness decreases rapidly due to the small value of G_i of the third and resistant soil layer.

5.2. Analysis of the dynamic tests from Limelette

The analysis is less complete than the previous one because the conclusions are similar. All the figures are not presented but the main ones are described and detailed in order to comment all the analysis.

The tests analysed have already been studied in chapter 3. It concerns the long prefabricated pile B8. The pile is 11 m long and its embedded part is 8.7 m long. The base is located at 9.5 m of depth.

The modelled pile is decomposed in 10 elements, the pile modulus of elasticity is fixed to 42000 MPa (c = 4140 m/s) and the surrounding soil is described by the input set of parameters (<u>Figure IV-12</u> to <u>Figure IV-14</u>). The exponents N of the velocity dependent power law are fixed to 0.2 for the shaft and 1 for the base according to literature. The ratio of shear modulus G_2/G_i describing the unloading is fixed to 1 and authorized to be optimised. Similarly to the SKW analysis, the input set of parameters is the same for each analysis but each blow is considered as an independent study.

The pile B8 was dynamically tested in 2002. the blows analysed are the blows #001, 002, 003, 007, 011 and 015. this sequence ensure a progressive increase of drop height from 0.4 m to 2 m. Each height is tested for the first time. They are called B8-00i. Table IV-7 informs of the chosen blows, of the drop heights and of the maximum and permanent settlements reached during each blow according to the analysis of the acceleration measurements at the pile top (more details in section 3.3 of chapter 3).

	Drop Height [m]	Max Settlement [m]	Perm Settlement [m]
B8-001	0.4 m	0.0033 m	0.0004 m
B8-002	0.6 m	0.0054 m	0.0005 m
B8-003	0.8 m	0.0062 m	0.0004 m
B8-007	1.2 m	0.0077 m	0.0004 m
B8-011	1.6 m	0.0094 m	0.0009 m
B8-015	2 m	0.0119 m	0.0039 m

Table IV-7: Summary of the analysed blows and of the reached settlements

The back-analysis is processed by the automatic algorithm proposed in this research and the following results are obtained. The matching procedure is performed by optimisation of all the parameters in the same time: since it is possible to refine the optimisation procedure to a certain number of parameters, Table IV-8 informs about the concerned parameters: 24 parameters.

Shaft (x 5 layers) :	$\tau_{ult,i}$	z_i	E_i	Js_i	G_2/G_1
Base 1 layer :	$\sigma_{ult,i}$	E_i	Js_i		

Table IV-8: List of optimised parameters

The optimisation procedure starts with a radius Δ of 90%. There are 10 reductions authorized and the last radius analysed is 5%. The number of iterations/radius without improvement of the matching quality factor D(p) is fixed to 100. The matching is processed on a duration of 25L/c which is longer than for the clay because the sand dampens less the signals (see Figure IIV-53 and Figure IIV-60). Table IV-9 contains the results of the matching procedure: D(p) is listed in %.

	Matching factor [%]	Max base settlement [m]	Difference max settlements pile top & base [m]
B8-001	0.74 %	0.0017 m	0.0016 m
B8-002	0.98 %	0.003 m	0.0024 m
B8-003	0.89 %	0.0035 m	0.0027 m
B8-007	1.18 %	0.0049 m	0.0028 m
B8-011	1.2 %	0.0063 m	0.0031 m
B8-015	0.91 %	0.0094 m	0.0025 m

Table IV-9 : Result of the matching procedure (matching quality factor D(p)) and maximum base settlement obtained for each test

Figure IV-73 to Figure IV-75 display the result of the matching procedure in terms of force-settlement curves for three analysis: B8-001, B8-007 and B8-015 corresponding to the drop heights of 0.4 m, 1.2 m and 2 m. The measured curve (Force measured – Set calculated) is compared to both calculated: "Force measured – Set calculated" and "Force calculated – Set measured". The matching is successful for all blows (see Table IV-9). Nevertheless, it can be pointed out that the calculated settlement curves (based on the force signal as input) fit much better with the reference curves than the calculated force curves (based on the settlement as input). There is a gap between those two curves between the maximum force and the maximum settlement (especially in Figure IV-74). The maximum and final settlement are conserved and the second peak of force is also well modelled (Figure IV-75). The matching is performed until stabilisation of the pile (about 25L/c).

The settlement behaviour of the last element close to the pile base (Table IV-9) does not show a constant behaviour like for the site of Sint-Katelijne-Waver but an upwards trend with the drop height and with a decreasing rate: the maximum settlement increases like the shortening of the pile's element (except for the last test #015). Consequently, the transfer of load to the base is also increasing and the mobilization of the shaft friction is not complete but tends to be.

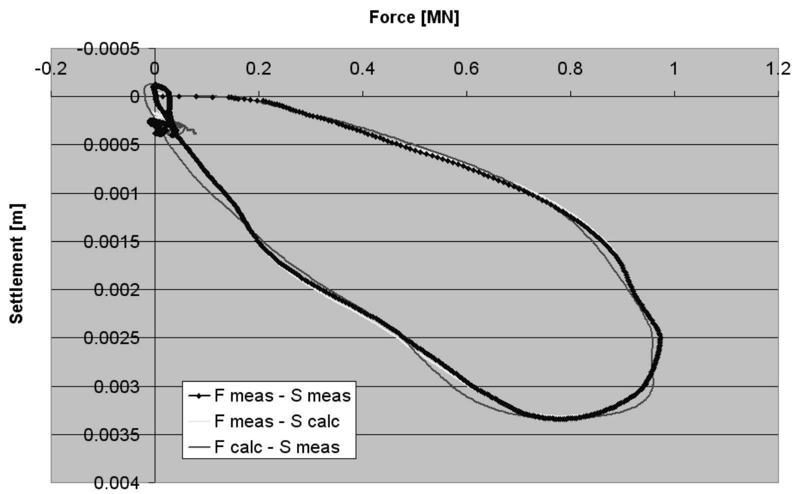

Figure IV-73 : Force-settlement curves (measured, and optimised (2 curves)) – blow B8-001/ 0.4 m

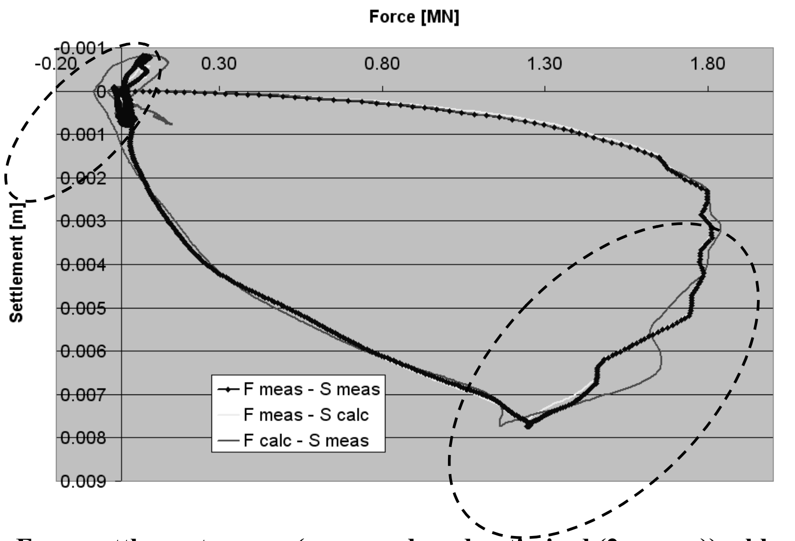

Figure IV-74 : Force-settlement curves (measured, and optimised (2 curves)) – blow B8-007/ 1.2 m

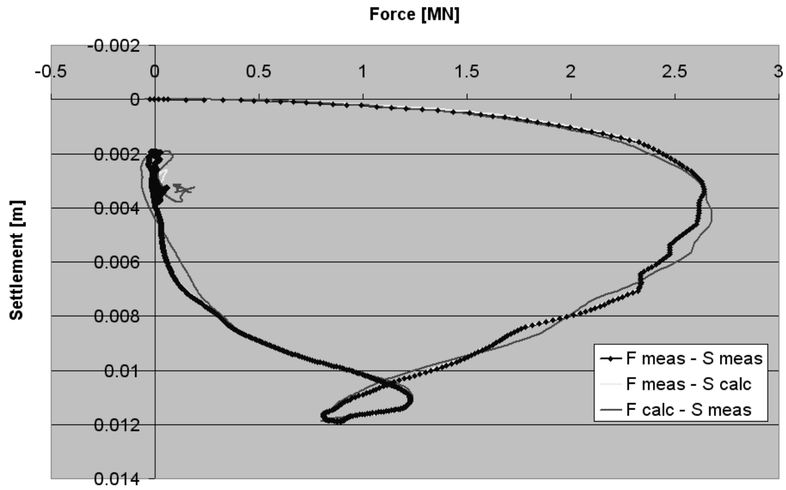

Figure IV-75 : Force-settlement curves (measured, and optimised (2 curves)) – blow B8-015/ 2 m

Figure IV-74 shows a good matching between curves, but there are two parts of the "Force Measured – Set calculated" curve that do not fit very well. The first one is systematic in the other analysis and correspond to the part of the curve between both maximum of measured force and settlement where the velocity is positive and decreasing (positive effect on the measured force) and the acceleration is negative (negative effect on the measured force). The second is also typical but corresponds to the part of the signal where the load has reached a quasi nil level and not the velocity (and consequently the settlement). The matching is difficult in this portion and is a question of radiation, essentially. The velocity curves matching (Figure IV-76) is also of very good quality except for the local maximum and minimum where a small gap exist. The first dashed ellipse on Figure IV-74 is located in the first decrease of the velocity (H = 1.2 m) marked with a grey arrow. The measured velocity presents a little threshold not modelled by the calculated curve.

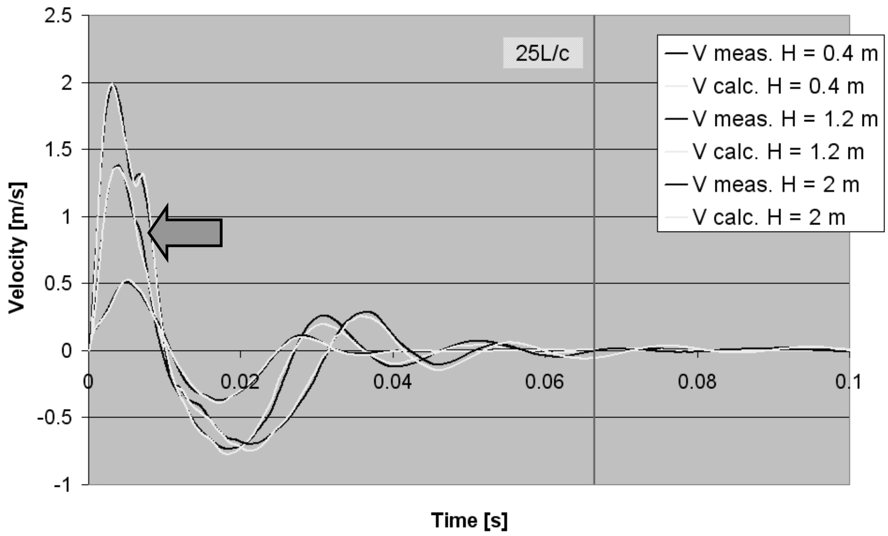

Figure IV-76 : Velocity curves (measured, and optimised) – blow B8-001/ -007 & 015

Figure IV-77 summarizes the data of the base parameters for the 6 blows analysed:

- The maximum reached stresses increase with the drop height denoting an increasing base mobilization. The range is from 0.3 MPa to more than 7 MPa;

- The ultimate soil resistance fluctuates between 12.26 and 22.46 MPa, but since the real stress mobilized reaches only max 53% of this value, the variability can be accepted. Moreover, an equilibrium exist with the initial elastic modulus to respect the settlement path of the pile base;

- The initial elastic modulus E_i reaches very high values, unrealistic and not physical (> to 2500 MPa). The reason is the same than for the previous analysis on the Sint-Katelijne-Waver data, there is an obligation to respect the settlement path and the load balance imposed as input and transmitted into the pile. Since this parameter is manifestly too high, the proposed values for σ_{ult} and σ_{max} are uncertain;

- The base damping factor J_b starts the sequence with a very high value (> 2.9 s/m) and decreases to stabilize for the higher drop height to about 0.85… 0.9 s/m; this value does not concern the ultimate soil resistance limit, but only the viscous term definition;

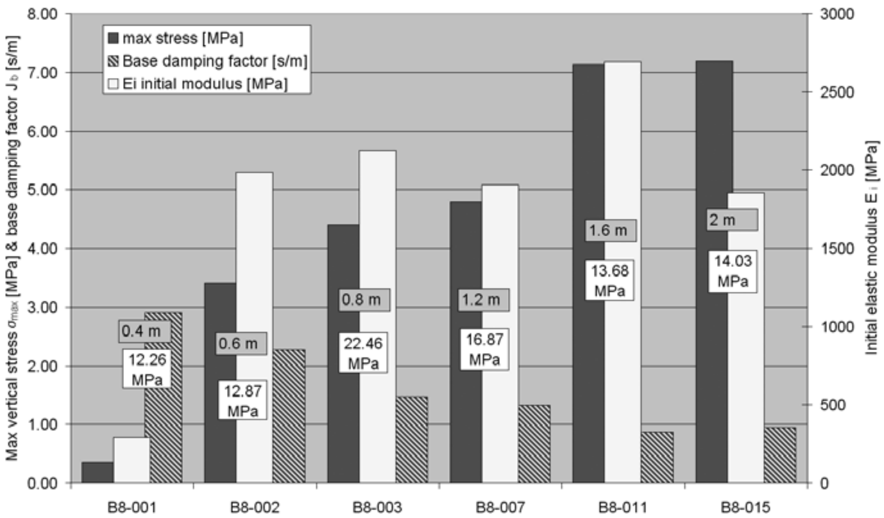

Figure IV-77 : Description of the base parameters after optimisation

The next three figures (Figure IV-78 to Figure IV-80) summary the soil reaction along the pile shaft with one sole figure per analysis. only the the blows #001, 007 and 015 are resumed (0.4 m, 1.2 m and 2 m respectively). The following information is available into the figures.

- The profile of the local shear strength f_s measured with the CPT;

- The step profile introduced as input (in dashed lines) τ_{ult};

- The step profile of the ultimate shear strengths obtained after optimisation τ_{ult};

- The step profile of the maximum reached shear stresses along the pile shaft τ_{max};

- The values of the initial shear modulus G_i for each soil layer;

- The value of the shaft damping factor J_s corresponding to each soil layers.

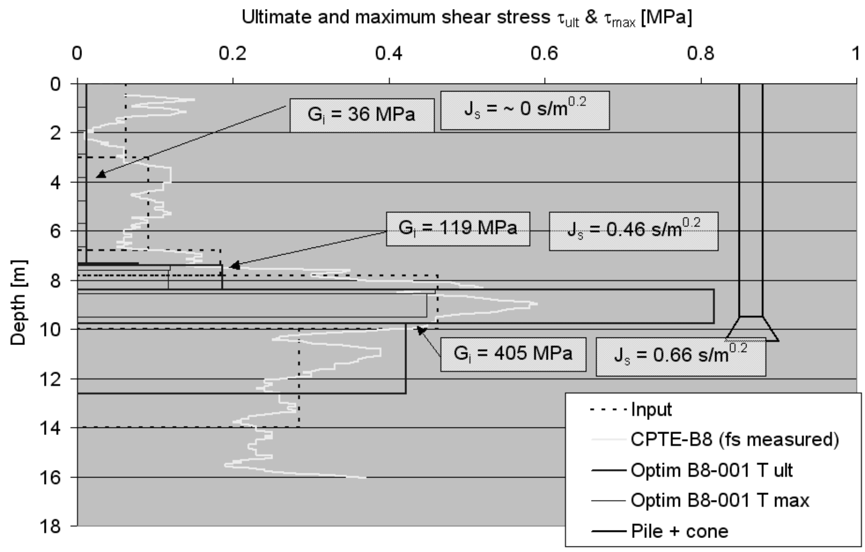

Figure IV-78 : Summary of the parameters of the soil reaction along pile shaft for the blow B8-001

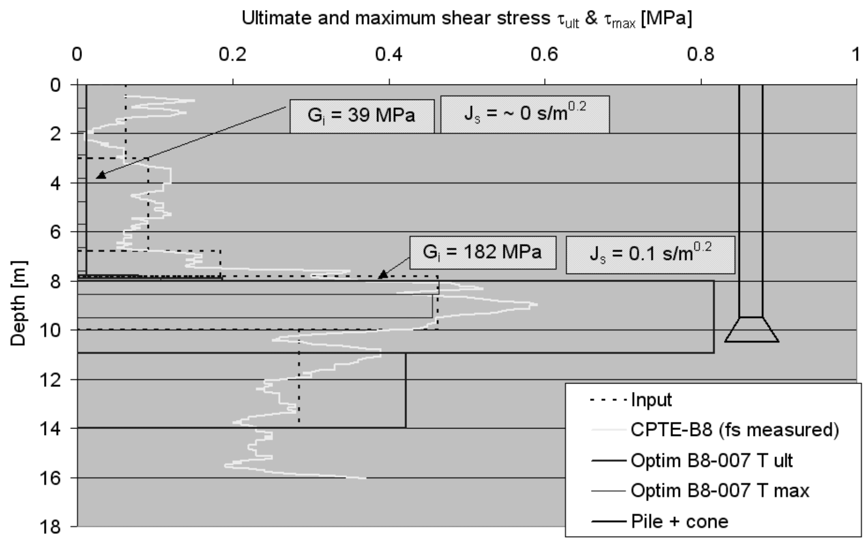

Figure IV-79 : Summary of the parameters of the soil reaction along pile shaft for the blow B8-007

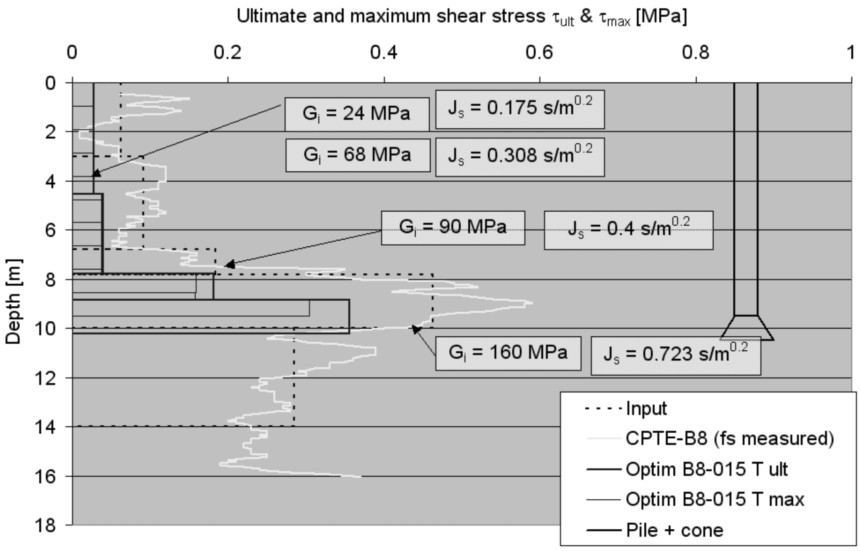

<u>Figure IV-80</u> : Summary of the parameters of the soil reaction along pile shaft for the blow B8-011

The following remarks can be enounced:

- The profile of the CPTE measurement f_s is respected. The layer of resistant sand in which the pile is embedded is found for all the piles. The optimisation process finds remarkably well the depths of soil resistance change of importance. However, the net ultimate values are not respected completely. The order of magnitude is ok, not the precise value. This is due to the settlement path to be respected and the balance existing between the stiffness and the resistance parameters that gives the shape to the hyperbolic curve;

- The first layer, until a depth of about 7.5 m defining the start of the sandy layer, is completely mobilized and also modelled inferior to the reference profile (f_s from CPTE); it is maybe due to the degradation of this weak layer or still an indirect consequence of the unloading shear modulus trouble; the last test (<u>Figure IV-80</u>) is slightly superior to the previous analysis but it is also shown that the sandy layer reaction has been reduced. There is a general equilibrium of the soil resistance along the pile in order to match the curves;

- The G_i profiles are more logical even if they present a downwards trend with the increasing drop height, the balance with the ratio G_2/G_i is less pronounced because the major part of the soil reaction is focused on the sandy layer close to the pile base. Hence, the balance between the modulus of the loading and unloading stages is performed on this sole layer and the initial shear modulus vary less than for the multi layers analysis of the clayed site. The values of the ratio of shear modulus (<u>Table IV-10</u>) exhibits a decreased trend with the drop height due to the fact that the maximum settlements to be respected increase with the soil mobilization but not the permanent settlement. Consequently, as observed on the <u>Figure IV-81</u>, the unloading modulus is adjusted to link both values.

	G_2/G_i
B8-001	0.46
B8-002	0.47
B8-003	0.4
B8-007	0.38
B8-011	0.25
B8-015	0.22

<u>Table IV-10</u> : List of unloading shaft ratio G_2/G_i

- Despite the fact that the poor first layer of soil is completely mobilized, there is no need of an added viscous reaction in most of the blows. All the first layer rheologic reaction is equivalent to a static reaction, the optimised values of J_{s1} can be equal to 0 s/m$^{0.2}$. The sandy layer presents a shaft damping factor that oscillates between 0.1 s/m$^{0.2}$ and 0.72 s/m$^{0.2}$. These values, and especially the last one, are confirmed by a sensitivity analysis around this position but are highly influenced by the optimised value of the ultimate soil resistance (τ_{ult} > 0.8 MPA for B8-007 and < 0.4 MPA for B8-015). Since the shaft damping factor mainly influences the rheologic soil reaction parameters into the ultimate formulation instead of the viscous one, the ultimate soil resistance has a strong influence. The real value of J is probably between 0.1 s/m$^{0.2}$ and 0.72 s/m$^{0.2}$ but need to be confirmed with a pile/soil system where the slippage is authorized and the troubles affecting the loading and unloading stiffness

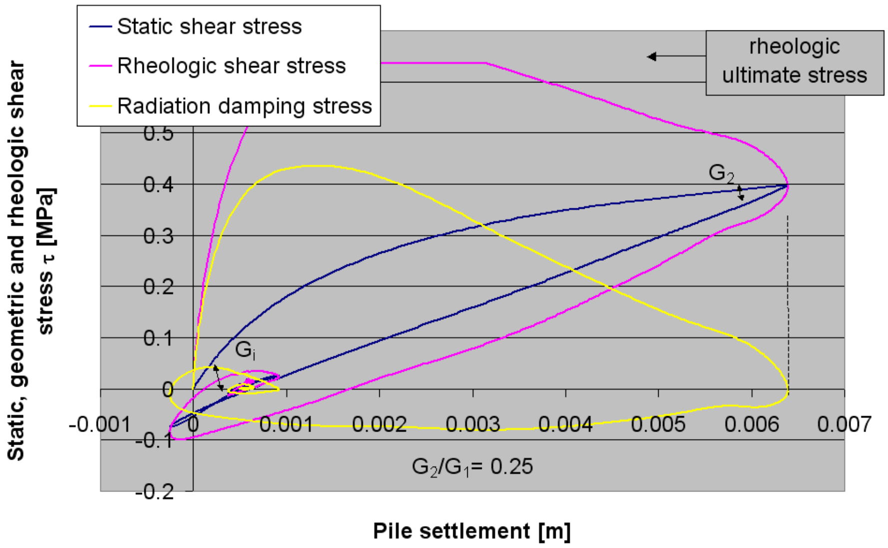

Figure IV-81 : Detail of the soil reaction along the 11th element of the pile (blow B8-011)

Figure IV-82 shows the detail of the settlements modelled of all the pile's elements for the blow B8-011 after optimisation. This is also the displacement path to be followed by each soil layer in contact with the pile's elements.

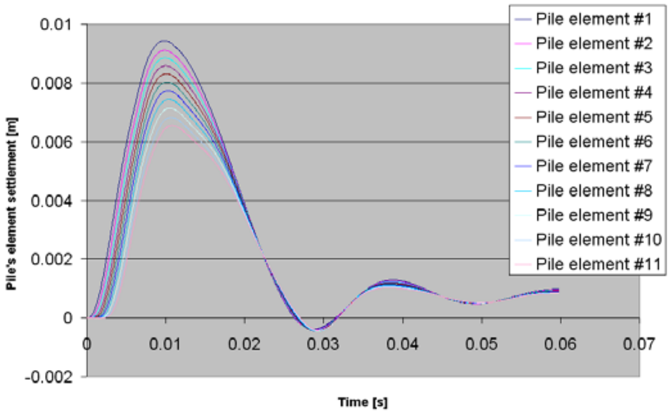

Figure IV-82 : pile's element settlement of B8-011

The trouble pointed out by the analysis of the Sint-Katelijne-Waver site still concerns the sandy site of Limelette. The need to dissociate both media, pile and soil becomes essential to perform a precise back analysis.

Similarly to the previous analysis, the integration of the maximum stresses reached during the blow along the pile and beneath the base (Figure IV-83) informs about the evolution of the shaft friction with depth and the last point adds the base to the shaft soil reactions. The first layer, described as of very small resistance gives a very poor soil reaction until the depth of 7.5 m. The same response is found for the 5 first analysis. Only the last one presents a more resistant soil reaction but this trend is balanced by a reduction of resistance in the sandy soil layer.

The figure highlights the quick mobilization of the shaft friction and the increasing mobilization of the base with the drop height.

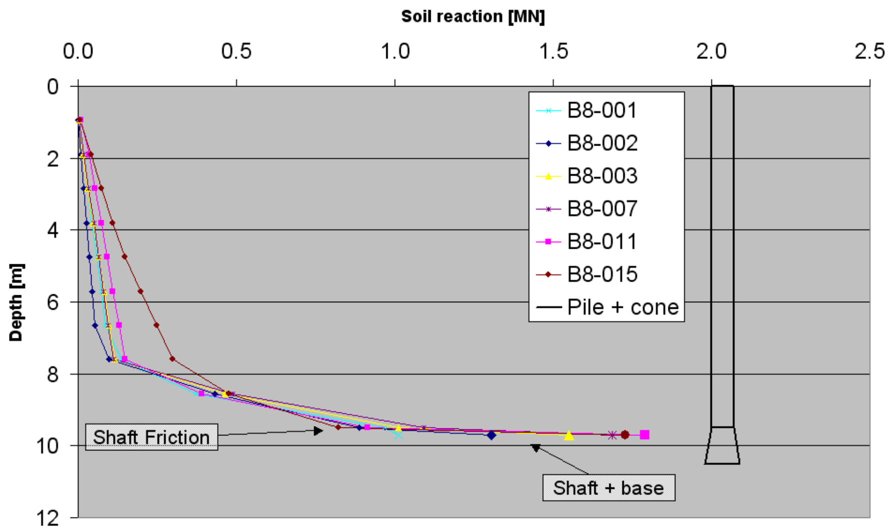

Figure IV-83 : Integration of the reached stresses along the pile and beneath the base for the analysis of Limelette

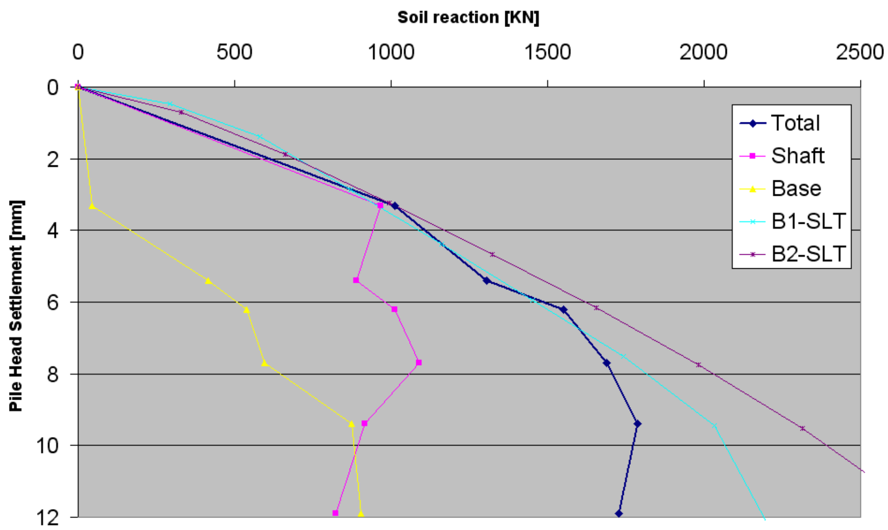

Figure IV-84 : Maximum mobilized load-maximum settlement curve for the sequence of blow B8 of Limelette

This evolution can be plotted vs. the maximum settlement measured of each blow (Table IV-7). Figure IV-84 exhibits this representation plus the separation of the total soil reaction in shaft and base components and the corresponding static load-settlement curves measured during the Static Load Tests performed on identical piles in the close vicinity of the pile tested dynamically (B1 & B2).

The initial stiffness agrees perfectly with the measured static curves. The shaft resistance is quickly fully mobilized (3.5 … 4 mm or 1% of the pile diameter) and the total shaft soil reaction is about 1 MN (oscillations around this value and equilibrium with the base reaction). The base reaction is increasing and is going to be superior to the shaft resistance as expected in sand. Since for the clayed site, the points corresponding to the large soil reactions are under-estimated compared with the SLT result, the same reasons than previously can be enounced.

Obviously, a general caution must be kept in mind with the likely influence of the modelling of the initial modulus and the loading and the unloading phases on the integrated soil reaction.

Finally, Figure IV-85 summaries the simulations of the static load-settlement curves obtained from the individual analysis. The settlement axis is limited to 10 mm what is the maximum settlement reached during the dynamic tests analysed. All the curves underestimate the static load settlement curves from both static load tests performed on the piles B1 and B2. The best fitted curve is the blow B8-003. the worst are the blows B8-001 and 015. If the first agrees perfectly with the SLT curves on the settlement mobilized (3.3 mm), it is not the case for the higher drop height blow.

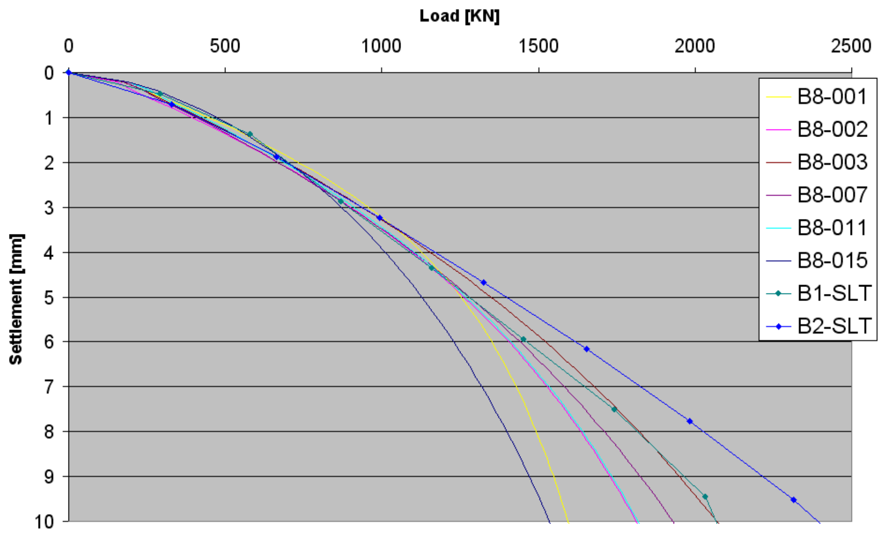

Figure IV-85 : Simulation of the static load-settlement curves based on the individual analysis of the B8 blows

6. Conclusions

This chapter is focused on the back analysis and the optimisation procedure used to analyse the dynamic measurements and to simulate the static load settlement curve to be compared with the measured one.

The principles of the matching procedure, the details and the requirements to have an objective and rapid method to perform it was presented: in order to have a better knowledge of the loading rate effect and especially on the parameters supposed to characterize it, all the parameters have to be optimised following a hierarchy based on of their relative weight.

The multi dimensional parameter perturbation sensitivity analysis developed by Berzi (1999) in order to explore the close vicinity about a point (defining a combination of n parameters in their R^n space) is used to systematically find the best combination improving the matching quality factor defining the matching process. When a new combination improving the matching is found, this value is set as new position of reference and a new perturbation analysis is undertaken until a stop criterion was achieved. The final combination is considered as the solution of the back-analysis.

This method is adapted to the back analysis of dynamic measurements from loading tests. The number of parameter to be optimised is free, and the solution can be tested by the sensitivity analysis in order to check its variability in its close environment. The consequences of this sensitivity on the simulated load settlement curves can be studied. This automatic procedure was tested and validated. The matching procedure converges.

The sensitivity analysis of the solution allows one to sort the parameters according to their relative weight in the matching procedure. Since the matching is successful and the combination converges towards the final solution, it is possible to refine in the later stages the less influential parameters by only selecting and optimising them. An analysis on the dynamic load test measurements from Sint-Katelijne-Waver and Limelette allows one to classify the rheologic parameters as not influential, except for the case where they are optimised together. The parameters leading the static soil reaction (τ_{ult}, thickness of the soil layers) appear to be leading the optimisation.

This automatic analysis was applied to the real data of the dynamic load tests of Sint-Katelijne-Waver and Limelette. The matching procedure is generally successful for all blows analysed. The back-analysis results are less reliable. The dynamic load tests analysis presents soil resistance profiles comparable to the CPT one (used as reference). The global static pile/soil response can be extracted and generally the simulated static load settlement curves are similar to the measured ones.

However, a systematic error hampers the optimisation of the loading and unloading initial shear moduli. Since the pile and soil motions are coupled by definition of the pile/soil system, the pile settlement path is imposed to the stress-displacement relationship of the soil. In order to match the measured and calculated curves of velocity, the constitutive soil relationships have to follow this settlement path. However, there is also a stress balance at each node of the pile/soil system between the rheologic soil reaction and the internal forces coming from the pile top. In order to fulfil this double constraint, the matching process influences the optimisation of the free parameters left in the soil-displacement relationship: the initial shear modulus for the loading and unloading stages and the rheologic parameters. Since the modulus influences greatly the stress generated for a given settlement, this parameter undergoes the consequences of the uncoupled behaviour of the pile and soil motions.

To avoid this trouble and to have a chance to succeed in the matching procedure and in the back analysis process, the slippage between pile and shaft must be authorized and both motions have to be independent during this slippage.

Nevertheless, except for the strict quality of the back analysis and despite the fact that there are some uncertainties on the results, there are some good results coming from the analysis of both sequences of DLT tests of the sandy and the clayey sites:

- The evolution of the soil mobilization with the drop height is as expected. First, the shaft friction mobilization, until a settlement of approximately 1% or 1.5% of the diameter where the shaft friction seems to be fully mobilized and afterward, progressively, the base reaction. The balance between base and shaft friction is also respected for the clayey and sandy sites;

- The soil mobilization integrated along the pile vs. the max settlement reached during dynamic load test is a comparable curve in stiffness, shape and quantity to the corresponding static load settlement curve.

- The profiles of soil resistance with depth are also recovered after the automatic processing;

- The rheologic parameters are more influential in the clayey site than in the sandy one. With the appropriate caution, it is possible the give a value to the shaft and base damping factors corresponding to the sites investigated (including the pile, the soil and the loading types):

	Sint-Katelijne-Waver	Limelette
Shaft damping factor	0.6 $s/m^{0.2}$	0.1 to 0.75 $s/m^{0.2}$
Base damping factor	1.75 s/m	0.9 s/m

- The simulations of the static load settlement curves agree with the measured one but are probably influenced by the pile/soil motion coupling.

On can observe a general balance in the soil reaction along and beneath the pile. The parameters of resistance, of stiffness and the rheologic parameters combine with each other to respect the settlement path all along the pile. The equilibrium at the base is particularly significant: both terms of soil reactions (shaft friction and base) combine to have a similar response submitted to the last pile element. This combination can have a strong influence on the optimised parameters value from base and shaft and an equivalent influence on the matching quality factor.

Finally, one can point out that the load rate effects are more developed in clay compared to sand. It can be observed that a good matching is not a sufficient condition to have good back-analysis results. Guides must orientate the matching. The first one and the most important one is the comparison with a good geotechnical information about the soil environment. Automatic guides can be implemented, but the most relevant is engineering judgement.